AIRS

Algorithm Theoretical Basis Document

Level 1B

Part 1: Infrared Spectrometer

Version 2.2i

10 November 2000

**H. H. Aumann, Dave Gregorich, Steve Gaiser, Denise Hagan,
Tom Pagano, Larrabee Strow and Dean Ting**

**Jet Propulsion Laboratory
California Institute of Technology**

File :ATBD1bir22i.doc

List of Tables

List of Figures

Changes since the Version 2.2g (11/10/00):

11/30/00 2.2.i p. 10 Moon avoidance in a 4 x 36 degree box starting at 70 degree from nadir
p. 16 Space view median algorithm

1. Introduction

The Level 1b Algorithm Theoretical Basis Document (ATBD) describes the theoretical bases of the algorithms used to convert the raw detector output (data numbers) from the Atmospheric Infrared Sounder (AIRS), the Advanced Microwave Sounding Unit (AMSU) and Humidity Sounder Brazil (HSB) to physical radiance units and, in the case of AIRS, perform in-orbit spectral calibrations. The description of the algorithms which convert the level 1b measurements to geophysical units is covered in the Level 2 ATBD.

The Level 1b ATBD for AIRS is divided into three parts:

- AIRS infrared spectrometer
- AIRS visible/near-infrared (VIS/NIR) channels
- AMSU/HSB Microwave channels.

This document is the ATBD for the level 1b processing of the AIRS infrared spectrometer. Level 1b algorithms perform the following functions:

1. conversion of scene measurements from engineering units to physical
2. estimation of detector noise,
3. estimation of the radiometric calibration accuracy
4. determination of the absolute spectral calibration and monitor spectral calibration stability.

Two reports related to the level 1b ATBD will issued in the year 2000:

1) The AIRS Calibration Report will include all data which define the AIRS instrument characteristics related to calibration. This report will include the final tables of coefficients required by the level 1b software.

2) The AIRS In-orbit Calibration Plan will define test sequences to be executed in orbit to optimize instrument performance.

The most up-to-date overall description of the AIRS instrument development is given in Ref.1. The AIRS Functional Requirements Document (FRD) is in Ref. 2. The AIRS Calibration Plan (Ref.3), dated 14 November 1997, contains a description of the relevant

parts of the AIRS instrument, calibration devices and calibration procedures for pre-launch characterization of parameters needed by the level 1b algorithms. The AIRS Validation Plan (Ref. 4.) describes post-launch validation of level 1b data using floating buoys, radio sondes, satellite- and aircraft-borne instruments. The AIRS home page at JPL and the Earth Observing System (EOS) project office at GSFC, http://www-airs.jpl.nasa.gov and http://eospso.gsfc.nasa.gov, respectively, post latest version of these plans.

Version 2.2 of the level 1b ATBD includes the following significant changes and additions from Version 2.1

1) The AIRS flight model calibration and validation phase was completed by 15 November 1999. Test analysis results as of 15 September 2000 are included. Key summary figures are included in the radiometric and spectral calibration appendices.

2) Details of the spectral calibration using upwelling radiance have been added

3) The Appendix includes a section on radiometric validation using a GCM to monitor radiometric bias.

4) The response to questions raised at February 1997 and March 2000 ATBD level 1b review have been revised to fit the revisions in ATBD text and additional information from the analysis of TVAC data.

.

1.1 Historical Perspective

The Atmospheric Infrared Sounder is a high spectral resolution IR spectrometer. AIRS, together with the Advanced Microwave Sounding Unit (AMSU) and the Microwave Humidity Sounder supplied by Brazil (HSB), is designed to meet the operational weather prediction requirements of the National Oceanic and Atmospheric Administration (NOAA) and the global change research objectives of the National Aeronautics and Space Administration (NASA). The AIRS flight model calibration started in November 1998 and was completed in November 1999. Integration onto the Aqua (formerly the EOS-PM1) spacecraft is scheduled to start in January 2000. The launch date for Aqua is 21 December 2000.

The High-resolution InfraRed Sounder (HIRS) and the Microwave Sounding Unit (MSU) on the National Oceanic and Atmospheric Administration (NOAA) polar orbiting satellite system have supported the National Weather Service (NWS) weather forecasting effort with global temperature and moisture soundings since the late 1970's. After analyzing the impact of the first ten years of HIRS/MSU data on weather forecast accuracy, the World Meteorological Organization in 1987 (Ref. 5) determined that global temperature and moisture soundings with radiosonde accuracy are required to significantly improve weather forecasts. Radiosonde accuracy is equivalent to profiles with 1 K rms accuracy in 1 km thick layers and humidity profiles with 20% accuracy in the troposphere. Advances in IR detector array and cryogenic cooler technology made this requirement realizable. AIRS is the product of this new technology. AIRS, working together with AMSU and HSB, forms a complementary sounding system for NASA's Earth Observing System to be launched in the year 2000.

The Interagency Temperature Sounder (ITS) Team, with representatives from NASA, NOAA, the University of Wisconsin and the Department of Defense (DOD) was formed in 1987 to convert the NOAA requirement for radiosonde accuracy retrievals to measurement requirements for an operational sounder. Instrument functional requirements established by this team in the areas of spectral coverage and resolution, calibration (radiometric and spectral), stability, spatial response (including alignment, uniformity, and measurement simultaneity), and sensitivity, became the basis of the AIRS Functional Requirements Document (Ref.2).

2. Infrared Spectrometer Description

2.1. Instrument Overview

The AIRS instrument and the devices and procedure used for the pre-launch calibration are described in the AIRS Calibration Plan, (Ref.3). In the following we describe those AIRS spectrometer design aspects which relate directly to the in-flight radiometric and spectral calibration activities and/or pre-launch calibration activities in support of the calibration software.

The AIRS instrument includes an infrared spectrometer and a visible light/near-infrared photometer. (The visible/near-IR photometer is discussed in Part 2 of the AIRS level 1b ATBD). The AIRS infrared spectrometer employs two multi-aperture slit and is pupil-imaging, with spectral coverage from 3.74 to 4.61 μm, from 6.20 to 8.22 μm, and from 8.8 to 15.4 μm. The nominal spectral resolution $\lambda/\Delta\lambda = 1200$. The spectrum is sampled twice per spectral resolution element for a total of 2378 spectral samples. A diffraction grating disperses the radiation onto 17 linear arrays of HgCdTe detectors in grating orders 3 through 11. The position of the dispersed beam on the focal plane in the dispersed and in the cross-dispersed direction can be accurately controlled by pivoting the collimation mirror using the Actuator Mirror Assembly (AMA). There are no plans to routinely move the AMA, once the setting is optimized during the on-orbit checkout of AIRS.

Spatial coverage and calibration targets are provided by the scan head assembly, containing the scan mirror and calibrators. The scan mirror motor has two speed regimes: During the first 2 seconds it rotates at 49.5 degrees/second, generating a scan line with 90 ground footprints, each with a 1.1 degree diameter FOV. During the remaining 0.667 seconds the scan mirror finishes the remaining 261 degrees of a full revolution. Routine calibration related data are taken during this time. These consist of four independent views of Cold Space View (CSV), one view into the Onboard Blackbody Calibrator (OBC), one view into the Onboard Spectral Reference Source (OBS), and one view into a photometric calibrator for the VIS/NIR photometer.

The IR spectrometer is cooled by a two stage radiative cooler. The temperature of the spectrometer is monitored with 6 fully redundant temperature sensors.

The temperature of the spectrometer is fine-controlled by a temperature servo in combination with a 2.8 watt heater at a set point to within 0.03K.

The servo heater can raise the spectrometer temperature set point by a maximum of 7 degrees above the natural orbital conditions, expected to be between 145K and 160K. The operating temperatures of the spectrometer is expected to be controlled at the start of the mission at a set point between 149K and 161K. The optimal set point will be determined during the on-orbit checkout. Full radiometric and spectral calibrations have been carried out during testing in the

AIRS Test and Calibration Facility (ATCF) at 149K, 155K and 161K. These measurement show excellent radiometric and spectral calibration stability, due to the a-thermal design of the AIRS (the optical bench and grating are made from a single billet of specially annealed Aluminum.). The measurements also have confirmed the 20 hour thermal time constant of the spectrometer.

The scan mirror rotates through 360 degree every 2.667 seconds. This produces data for one scan line with 90 footprints on the ground and 6 calibration related footprints. The scan mirror is cooled by radiative coupling to the cold IR spectrometer, resulting in a mirror temperature approximately 100K warmer than the spectrometer temperature. The scan mirror temperature is monitored by a non-contacting sensor located at the base of the rotating shaft, about 6" from the scan mirror surface. The temperature gradient between the scan mirror surface and the temperature sensor is estimated to be less than 0.5K and temperature gradient across the scan mirror surface is less than 0.05K. The scan mirror is coated with silver, overcoated with a protective layer of SiO_2 by Denton using a proprietary process. The scan mirror temperature, mirror angle (relative to nadir), emissivity, emissivity non-uniformity and polarization are part of the radiometric calibration algorithm.

2.2. Calibration Devices.

Routine IR radiometric calibration related data are taken while the scan mirror rotates from -49.5 degrees (relative to nadir) through 180 degrees (anti-nadir position) to +49.5 degrees. These data consist of four independent views of cold space (CSV) and one view into the Onboard Radiometric Calibrator (OBC) source. The view into the Onboard Spectral reference source (OBS) once per scan line is used only during ground-testing. In-orbit the upwelling spectral radiance for the nadir footprints is used for the spectral calibration. The AIRS spectrometer is pupil imaging, i.e. detectors are located at a pupil stop of the spectrometer optics (as opposed to the detectors being at a field stop, i.e. imaging the scene on the detectors). This insures that spatial non-uniformity in the radiance emitted by the calibration source and/or the scene does not contribute to the spectral or radiometric calibration error.

Onboard Radiometric Calibrator (OBC): The OBC is a deep wedge cavity blackbody with a rectangular 5.7 cm by 9.5 cm clear aperture. The depth of the blackbody cavity is twice the diagonal of the clear aperture. The blackbody housing and cavity are made from beryllium to reduce its mass to 2 kg. The surface of the OBC wedge cavity is coated with paint with emissivity higher than 0.91. This allows multiple bounces of the light within the cavity. The OBC effective emissivity starts at 0.999 and degrades at end-of-life to no less than 0.993.

Four semi-conductor resistance temperature sensors, T1..T4, monitor the temperature at key positions to an accuracy of 0.1 K. T1 and T2 are located on the sloping part of the wedge, T3 is located on the vertical part of the wedge, and T4 is located at the outside aperture of the OBC.

The four temperature sensors in the OBC are fully redundant. If a temperature sensor is found to be outside the nominal limits, a flag is raised, indicating that the calibration accuracy may be compromised. Switch-over to the redundant sensor requires verification of the condition by the data monitoring team on the ground and uploading corrective action. Since the OBC temperature has been extremely stable during the entire ATCF testing, the level 1b algorithm continues with the data processing using the nominal OBC temperature. The OBC is analog servo controlled at 308.0 +/- 0.01K.

The effective temperature and emissivity of the OBC was calibrated using a Large Area Black Body (LABB). The output of the LABB is NIST traceable through it Platinum Resistance Thermometers (PTM). This is discussed in Appendix 3.

Cold Space View (CSV): There are four consecutive views of cold space center at 75.3, 83.3. 91.6 and 100.2 degrees from nadir, named S3, S4, S1 and S2, respectively. Since the scan mirror moves continuously, the effective area used for the CSVs starts at 71.8 degrees and ends at 104.5 degrees from nadir. The measured off-axis rejection is 10^{-3} or better at 0.8 degrees, 10^{-4} or better at 2 degree from the AIRS optical axis on all channels. Any significant source of thermal emission inside a 4 x 36 degree box starting at 70 degree will cause an undesirable shift in the CSV. There are two potential source: The effective Earth horizon (100km above the surface) from the 705 km altitude orbit is at 64.4 degrees, and the Moon. Although the Earth horizon is more than five degrees from the 10^{-4} response contour, it may make S3, the CSV nearest to the horizon, permanently unusable. This will be determined empirically during the on-orbit testing. The Moon signal may contaminate one or at most two of the CSVs no more than once per month during several consecutive scan lines. The resulting increase in the CSV signal ranges from imperceptible at the noise level to 10% of full scale, i.e. 6000 data numbers. Although this condition is predictable from the boresight and Moon ephemeris data, the AIRS level 1b algorithm eliminates CSVs with lunar contamination without the ephemeris data.

Onboard Spectral reference source (OBS): A mirror coated with a thin film (about 100 microns thick) of Parylene is used as the On-Board Spectral reference source (OBS) for routine testing of spectrometer functionality pre-launch only. Figure 2.1 shows the spectrum from two tests separated by 24 hours. Although the spectral features are fairly broad, results from the thermal vacuum testing indicate that the OBS allows measurements of relative spectral shifts with repeatability of the order of 1% of the width of the spectral response function. The locations of the nine usable spectral features are listed in Table 2.1. The in-orbit spectral calibration using the accurately known features in the upwelling spectral radiance as discussed in section 4.3.

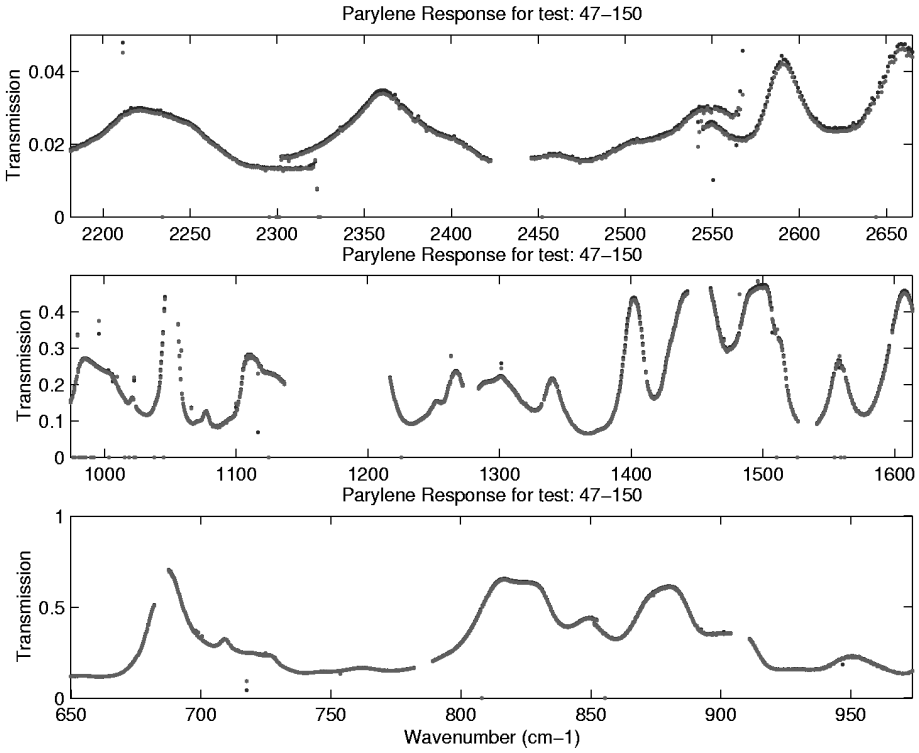

Figure 2.1. OBS spectra obtained during ATCF testing at the start and the end of the 24 hour orbital heat load simulation test.

Spectral Feature Location	Array location		Spectral Feature Location	Array location
709 cm^{-1}	M11		1233 cm^{-1}	M4d
970 cm^{-1}	M7		1327 cm^{-1}	M4c
1032 cm^{-1}	M6		1340 cm^{-1}	M3
1607 cm^{-1}	M4a		1402 cm^{-1}	M3
			1417 cm^{-1}	M3

Table 2.1. OBS Spectral Feature locations.

3. Radiometric Calibration

The AIRS spectrometer has 2378 spectral channels grouped in seventeen arrays. The first 15 arrays use PV detectors, the last two use PC detectors. The AIRS level 1b software reads the raw output of each of the 2378 channels (level 1a) for each footprint and converts it to a calibrated radiances using the AIRS radiometer calibration equation. In the following section we discuss the radiometer calibration equation (algorithm) and estimate the accuracy of the calibration. Details of the derivation of the key calibration parameters are presented in Appendix 3.

The absolute radiometric calibration accuracy of each AIRS spectral channel, as stated in the AIRS Functional Requirements document (Ref.2.), is the larger of 3% of the radiance or 4*NEN, over the full dynamic range of AIRS from 190K to 325K, where NEN is the Noise Equivalent Radiance. Since brightness temperature uncertainties are more useful than radiance uncertainty for a temperature sounder, most of the results are expressed as temperature uncertainty. The table in Appendix 5 lists the temperature change, which corresponds, to a 1% change in radiance as function of scene temperature.

The level 1b software routinely generates Level 1B quality assessment indicators. These indicators are used for off-line trend analysis and are also passed on to the level 2 (geophysical product generation) software for product accuracy estimation.

3.1. Radiometer Calibration Equation

A primary function of the Level 1B software is to convert the Level 1A digital numbers into calibrated radiances. All digital numbers in the 90 Earth view footprints are converted to radiance units. The conversion uses the AIRS radiometer calibration equation given below.

$$N_{sc,i,j} = \frac{a_o(q_j) + a_{1,i}(dn_{i,j} - dn_{sv,i}) + a_2(dn_{i,j} - dn_{sv,i})^2}{1 + p_r p_t \cos[2(q_j - d)]} \qquad \text{Eq 3-1}$$

where

$N_{sc,i,j}$ = Scene radiance of the i^{th} scan and j^{th} footprint (mW/m^2-sr-cm^{-1})

i = Scan Index

j = Footprint Index (1 to 90)

θ = Scan Angle. θ = 0 is nadir.

$dn_{i,j}$ = Raw Digital Number in the Earth View for the i^{th} scan and j^{th} footprint

$dn_{sv,i}$ = Space view offset. This is an algorithmic combination of the 4 AIRS raw space view digital numbers.

a_o = Radiometric offset. This is nonzero due to polarization and is scan angle dependent.

$a_{1,i}$ = Radiometric gain. This term converts dn to radiance based on the radiometric gain as determined using the OBC blackbody.

a_2 = Nonlinearity Correction. This term is determined pre-flight based on linearity data from the LABB.

$p_r p_t$ = Polarization Product. This is the product of the polarization from the scan mirror and the spectrometer.

δ = Phase of the polarization of the AIRS spectrometer (zero at launch).

3.1.1 In-orbit gain determination

The gain is the first order responsivity of the AIRS in terms of radiance units (mW/m^2-sr-cm^{-1}) per digital number (dn) measured from the instrument. The gain, derived directly from Eq. 3-1, is calculated as follows:

$$a_{1,i} = \frac{N_{OBC,i}(1 + p_r p_t \cos 2\delta) - a_o(q_{OBC}) - a_2(dn_{obc,i} - dn_{sv,i})^2}{(dn_{obc,i} - dn_{sv,i})} \qquad \text{Eq 3-2}$$

where the new terms are

$a_{1,i}$ = Gain of the AIRS per scan in units of Radiance per digital number, (N/dn).

$N_{OBC,i}$ = Radiance of the on-board calibrator blackbody (OBC BB) as calculated below.

$a_o(\theta_{OBC})$ = Radiometric offset evaluated at the angle of the scan mirror while viewing the OBC at 180° per the equation defined in the following section. Units of Radiance, N.

a_2 = Second order coefficient as obtained from pre-flight testing (N/dn^2)

$dn_{obc,i}$ = OBC Blackbody digital number for the i^{th} scan

The OBC Radiance is calculated using the 4 thermistors. The radiance of the OBC, $N_{OBC,i}$ is defined as

$$N_{OBC,i} = \varepsilon_{OBC}\, P(T_{OBC,i}) \qquad \text{Eq 3-3}$$

where ε_{OBC} is the effective OBC emissivity , P is the Planck blackbody function evaluated at the wavelength of each channel and T_{OBC} is a single values for all channels calculated from

$$T_{OBC} = \tau_1 T_1 + \tau_2 T_2 + \tau_3 T_3 + \tau_4 T_4 + \tau_5 T_5 \qquad \text{Eq 3-4}$$

where $T_{1,2,3,4}$ are obtained from the instrument telemetry. T_5 = 0.3K from the pre-flight calibration, $\tau_{1,2,3,4,5}$ are constants based on the pre-flight calibration of the OBC using the LABB. The algorithm for calculating the OBC blackbody radiance allows correction for uncertainties observed in orbit due to the surrounding environment at some later date without rewriting the software.

The level 1b software calculates a_1 for each detector for every scan line. After 135 scan line the software calculates the mean gain and the standard deviation of the gain. The mean gain is used in the radiometric calibration equation 3-1. The standard deviation of the gain is an estimate of detector NEN for a 308K scene, NEN_{308K}. This value is converted to the NEDT and passed stored with the calibrated data.

3.1.2. Space-View-Processing

The signal measured by AIRS viewing a ground target is the combination of the target radiance, the thermal emission from the AIRS instrument and electronics offset. The data number associated with a thermal emission and electronics offset is determined by means of the Cold Space Views (CSV). As discussed in Section 2.2 AIRS takes four space view measurements: S3, S4, S1 and S2, respectively while the AIRS boresight vector moves from 71.8 to 104.5 degrees from nadir.

S3b, S4b, S1b, S2b, OBC, (….. scan line with 90 scene views…..) S3a, S4a, S1a, S2a.,

where S3b is the before the scan line and S3a is after the scan line. The effective Earth horizon is at 64.4 degrees from nadir. These space view measurements are followed by a view of the OBC at 180 degree scan angle. The cycle repeats every 2.67 seconds. The space view processing algorithm which converts the four space views into the optimum, DN_{space} for the 90 scene views and the OBC view is a compromise between simple, reliable, and not bad and complex, needs tuning in orbit and very good. The ready-at-launch algorithm is the former. At launch + 4 month a transition will occur to a more complex algorithm.

3.1.2.1 Launch-ready algorithm.

The launch-ready algorithm produces an estimate of the cold-space view which is accurate to within the detector NEDT, except for infrequent cases of Moon interference, where the entire scan line is identified as “radiometrically out of spec”.

If the Moon is located close to or in the AIRS field-of-view during one of the cold-space-views the output of that space view will to go up for all PV channels and down for all PC channels.

For each channel and each scan line the algorithm calculates four parameters: DN_{space}, SV_number, Range_ DN_{space}, and SV_range_flag.

DN_{space} = median (S3b, S4b, S1b, S2b, S3a, S4a, S1a, S2a)

SV_number = number of the median space or the spaceview just below the median in case of an even number of views.

Range_ DN_{space} = max (S3b, S4b, S1b, S2b, S3a, S4a, S1a, S2a)

-min(S3b, S4b, S1b, S2b, S3a, S4a, S1a, S2a).

SV_range_flag = 0 if (Range_ DN_{space} < 6 * NEDT) else = -1

If SV_range_flag =-1 the scan line is flagged as "radiometrically out-of-spec" for that detector.

Space View Performance estimate:

1. Under nominal conditions the eight space views used for the calculation will be distributed like gaussian random numbers, i.e. Error_ DN_{space} = NEDT / root(8) << NEDT.
2. If the Earth horizon consistently interferes with S3, such that SV_range_flag <> 0, then the algorithm will produce a space view value with Error_ DN_{space} < NEDT. Since the NEDT is typically in the 0.2K – 0.4K this is very acceptable during the on-orbit validation period. Should this condition be true, then the algorithm will be modified to delete S3.

   DN_{space} = median (S4b, S1b, S2b, S4a, S1a, S2a),

   with Error_ DN_{space} = NEDT / root(6) < NEDT.
3. If the Moon contributes significantly to one of the space views, then the algorithm flags the scan line as SV_range_flag =-1 . If S3 is horizon contaminated and has not been deleted as a usable space view, and assuming S1 is degraded by the Moon,

   DN_{space} = sorted (S4b, S2b, S4a, S2a, <u>S3a, S3b,</u> <u>S1a, S1b</u>)

   = mean (S2a, <u>S3a</u>) , i.e bad and SV_range_flag =-1.

   If S3 has been removed from the algorithm then

   DN_{space} = sorted (S4b, S2b, S4a, S2a, <u>S1a, S1b</u>) = mean (S4a, S2a) , i.e. the average of two good space views, although SV_range_flag =-1. The outliers CSVs are shown underscored.

4. In the rare case that the Moon contributes significantly to two space views, say S1 and S2,

   DN_{space} = median (S4b, S1b, S2b, S4a, S1a, S2a) = sorted (S4b, S4a, S2b, S2a, S1a, S1b)

   = mean (S2b, S2a) and SV_range_flag =-1.

   i.e. the space view is bad. Given the infrequent of this event, this is acceptable.

3.1.2.2. Advanced space view algorithm

The launch ready algorithm is a compromise between simplicity and reliability. Several considerably more complex algorithm are being bread-boarded, where space view weights c_1, c_2, c_3, and c_4 are used to reject or limit the contribution of any particular space view sample from the determination of the optimum DN_{space}. Their value will be determined in orbit during the checkout phase by gathering statistics of the relative amplitudes of the four space views. The advanced algorithms may also use the lunar ephemeris to identify space views with likely Moon contamination. An additional augmentation under evaluation is to time interpolate between the space views at the start and the end of every scan line in order to minimize noise due to short term drift.

3.1.2.3 DC Restore

The analog output of each detector is periodically clamped by the electronics to voltage V_o at the end of the dwell period associated with viewing space view #4, but before space view #1. Since V_o has been set pre-launch to about 10% of the dynamic range by a resistor, based on experience acquired during the calibration and characterization phase, as a zero offset of the analog-to-digital converter (ADC), the discontinuity between S4a and S1a is about 1000 DN (depending on the particular channel). The value of V_o does not enter the calibration equation. This event, referred to as the DCR ("DC Restore"). The discontinuity is due to changes in the detector background and electronics offset since the last DCR. While the time of the DCR, which occurs every 18 (TBD) minutes, is identified in the downlink telemetry, the ready-at-launch algorithm produces an acceptable estimate of the space view and a flag without the need to identify the DCR time in the data record.

Assuming S3a and S3b are Earth contaminated we get

DN_{space} = median (S3b, S4b, S1b, S2b, S3a, S4a, S1a, S2a)

= sorted (S1b, S2b, S2a, S4a, S1a, S3a, S4b, S3b)

= mean (S4a, S1a).

Since S4a and S1a are both good, DN_{space} is the average of two good space views. At the same time the SV_range_flag =-1 which identifies the entire scan line as radiometrically out-of-spec. Given the infrequent of this event, this is acceptable.

3.1.3. Scan Angle Dependent Radiometric offset

The AIRS radiometer calibration equation includes a scan angle dependent radiometric offset term proportional to the amount of polarization of the scan mirror and the spectrometer

$$a_o(q_j) = N_m \bullet p_r p_t \bullet [\cos 2(q_j - d) + \cos 2d] \qquad \text{Eq 3-6}$$

where

$a_o(\theta_j)$ = Scan angle dependent offset due to polarization (mW/m^2-sr-cm^{-1})

N_m = Radiance of a Unity Emissivity Surface at the Scan Mirror Temperature, T_{sm} obtained from the telemetry as indicated below and the Planck blackbody equation.

$p_r p_t$ = Product of the polarization factor of the scan mirror and spectrometer respectively. (dimensionless)

θ_j= Angle of the scan mirror for the j^{th} footprint (0° is nadir)

δ = Phase of the polarization of the AIRS spectrometer.

Although the radiance from the scan mirrror at 250K is small, it cannot be neglected. Eq.3-6 was validated during prelaunch calibration. Details are given in Appendix 3. The fit to the observed data is excellent.

3. 2. Radiometric Calibration Error Estimation

We can determine the uncertainty in the radiometry by applying variance analysis on the radiometric transfer equation, 3-1. This will give us only those errors which are directly attributable to the calibration equation. There are other potential errors discussed below which are implicit in the instrument and calibration approach that are covered in other sections.

We differentiate with respect to the primary uncertain variables in the radiometric transfer equation. All terms are uncorrelated and of type B (Ref. 11), except the SNR which is of type A. These are:

- uncertainty in the polarization product of the scan mirror and the spectrometer, $p_r p_t$,
- uncertainty in the temperature of the scan mirror, T_{sm},
- uncertainty due to the spatial nonuniformity of the mirror emissivity, ε_{sm},

- uncertainty in the gain correction term of the OBC, ε_{OBC} (relative to the LABB),
- uncertainty of the temperature of the OBC BB, T_{OBC},
- uncertainty in the nonlinear term, a_2, and
- the instrument noise, dn.

$$\P N_{SC}{}^2 = \left(\frac{\P N_{SC}}{\P p_r p_t} \Delta p_r p_t \right)^2 + \left(\frac{\P N_{SC}}{\P T_{sm}} \Delta T_{sm} \right)^2 + \left(\frac{\P N_{SC}}{\P e_{sm}} \Delta e_{sm} \right)^2 + \ldots$$
$$\ldots + \left(\frac{\P N_{SC}}{\P e_{OBC}} \Delta e_{OBC} \right)^2 + \left(\frac{\P N_{SC}}{\P T_{OBC}} \Delta T_{OBC} \right)^2 + \left(\frac{\P N_{SC}}{\P a_2} \Delta a_2 \right)^2 + \left(\frac{\P N_{SC}}{\P dn} \Delta dn \right)^2 \quad \text{Eq 3-7}$$

First we differentiate equation 3-1 according to equation 3-7. Then we divide both sides of the equation by the scene radiance N_{SC} and simplify terms by approximating $N_{SC}=a_1 dn$ and we get the relative radiometric uncertainty.

$$\left(\frac{\P N_{SC}}{N_{SC}} \right)^2 = \left(2 \frac{N_m}{N_{SC}} \bullet \cos 2(q_j) \Delta p_r p_t \right)^2 + \left(\frac{2}{N_{SC}} \frac{\P N_m}{\P T_{sm}} \bullet p_r p_t \bullet \cos 2(q_j) \Delta T_{sm} \right)^2 + \ldots$$
$$\ldots + \left(\frac{\Delta N_{sm}}{N_{SC}} \right)^2 + \Delta e_{OBC}{}^2 + \left(\frac{1}{N_{OBC}} e_{OBC} \frac{\P N_{OBC}}{\P T_{OBC}} \Delta T_{OBC} \right)^2 + \left(\frac{N_{SC}}{a_1{}^2} \Delta a_2 \right)^2 + SNR^{-2} \quad \text{Eq. 3-8}$$

3.2.1 Error Terms

$p_r p_t$: The first primary error term is the uncertainty in the product of the polarization factors of the scan mirror and spectrometer. Appendix 3 shows that we can obtain the product three ways; first using measurements of the polarization of the AIRS, second using measurements of the polarization of the components of the AIRS and a model, and thirdly from measurements of the radiometric intercept of the linearity data using the LABB. The uncertainty we choose to carry is the differences between the two extreme measurements, the system polarization and the component model.

? T_{sm}: The AIRS scan mirror temperature is monitored using a non-contacting temperature sensor located at the base of the rotating shaft as described in section 2.1 The uncertainty in the scan mirror temperature is estimated to be less than 0.5K by design. For this error analysis we have used 1K. The contribution is still negligible compared to the other terms.

? e_{sm}, ? N_{sm}: The AIRS scan mirror may have some spatial non-uniformity that will cause an offset of the signal with scan angle that differs from that obtained while observing the OBC BB and space views. This is due to the way the AIRS detectors form an image on the scan mirror

rather than a pupil. We use initially an at-launch non-uniformity of 0.001 in emissivity. The end-of-life estimate and a derivation of this error is discussed in Appendix 3.

? e_{OBC}: A 0.3K offset was applied during the calibration to match the radiances of the OBC and the external LABB. The residuals are contained in the gain correction term, e_{OBC}. It is possible that the observed differences are due to how we view the OBC and the LABB and is not well understood. We therefore have included all of the gain correction as an error; i.e **? e_{OBC} = 1-e_{OBC}**. We calculate the gain correction as discussed in Appendix 3.

? T_{OBC}: The temperature of the OBC Blackbody is monitored by 4 temperature sensors located in and around the OBC as discussed in section 2.2. We have seen a fluctuations on the order of ±0.05K in the blackbody temperature and have allowed that entire observation to represent our uncertainty in this term.

? a_2: The uncertainty in the nonlinear term is obtained by observation of the channel-to-channel variance in this term. The nonlinearity and how we obtain this term are discussed in Appendix 3

SNR: The Signal-To-Noise Ratio is obtained by viewing a 250K source, the LABB, and calculating the mean and variance on the derived radiance.

3.2.2 Error Results

Figure 3.2 shows the results of predicting the radiometric errors based on the assumptions in the previous section. Overlaid on the prediction is the error resulting from an independent measurement of the LABB, taken three days after taking the data used to derive the calibration coefficients and taken at a different scan angle. The error is the difference between the derived temperature of the LABB using the calibration coefficients and the true temperature obtained from the LABB temperature sensors. Results show that we expect and have measured errors less than 0.1K for all but the longest wavelengths. We expect higher uncertainties at longer wavelengths due to greater uncertainties in the polarization product, $p_r p_t$.

Important Note: There are other radiometric errors that are not quantifiable pre-launch that may affect overall in-flight accuracy. These are discussed in the next section.

We have included all the errors discussed above except the SNR in this prediction. The SNR is a random error with zero radiometric bias (type A rather than type B) and for this reason does not produce a systematic uncertainty but a random uncertainty from sample to sample. The SNR is expressed as the NEdT at 250K and is plotted in Figure 3.3.

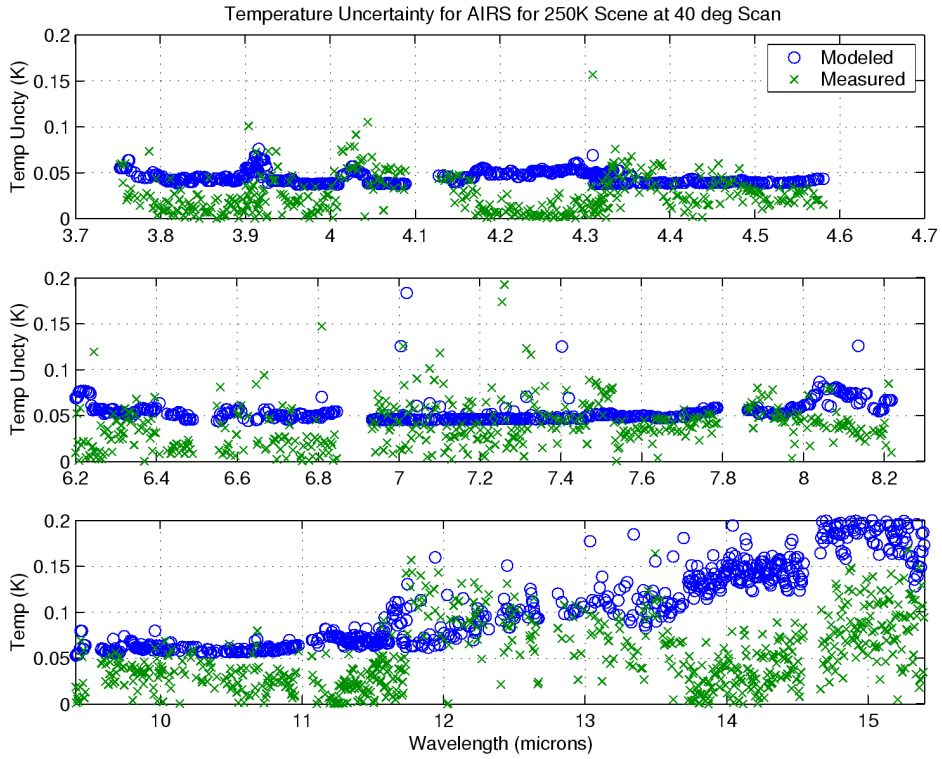

Figure 3.2. Radiometric error for AIRS while viewing a 250K scene. Measured errors were obtained while viewing same target, LABB, on different day at different scan angle. Does not include errors discussed in the next section. The radiometric errors (bias) are typically below the detector noise per footprint.

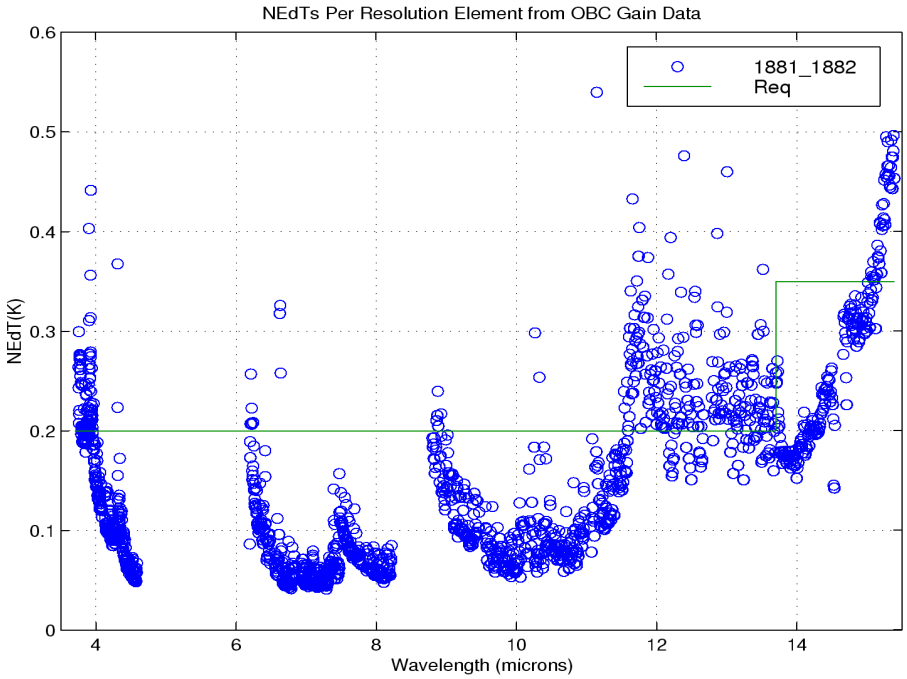

Figure 3.3. AIRS NEDT referred to a 250K scene. The radiometric errors shown in Figure 3.2 are bias values and are typically below the noise observed for one footprint.

3.2.3 Non-Quantifiable Pre-Flight Errors

Errors not included in the above equation are those that are not explicitly part of the radiometric equation. These errors are not quantifiable pre-flight through testing yet may affect flight calibration accuracy. They are as follows.

1) NIST transfer of the absolute calibration to the LABB. We expect this error to be a systematic error (bias) less than 1%. The LABB radiance is traceable to NIST through the temperature sensors of the LABB and analysis of the LABB design.

2) Degradation of the OBC effective output. Given the design of the OBC and its protected location, the likelihood of a measurable decrease in the output due to emissivity degradation is extremely small. The AIRS Validation program routinely monitors the radiometric calibration bias to an accuracy of about 0.1K to guard against this possibility. Details are presented in Appendix 7.

3) Radiometric error due to spectral response function uncertainty. This is a potential issue only in regions of high spectral scene contrast if either the SRF centroid position or the SRF effective width is in error. As long as both are known to within 1% of the SRF width, the radiometric error is less than one NEN. This is discussed in section 4.0

3.3. Detector noise estimation

The level 1b software routinely characterizes the gaussian noise amplitude and non-gaussian characteristics (if any) for each channel. This information is passed to the level 2 algorithm for use in the retrieval accuracy estimation.

1. Gaussian noise estimation

The level 1b software calculates a_1 for each detector for every scan line. After 135 scan line the software calculates the mean gain and the standard deviation of the gain. The standard deviation of the gain is an estimate of detector NEN for a 308K scene, NEN_{308K}. This value is converted to the NEDT and passed stored with the calibrated data.

2. Non-gaussian noise estimation.

Based on ATCF test analysis the output, dN , observed for successive space views for each detector is predictable to an accuracy approaching the gaussian noise for most detectors. The level 1b software makes use of this fact for quality control (QA) using the difference between space view data number between the begin and the end of each scan. Let $ds2_j$ be the observed difference between the change in space view 2 separated by one scan line for the j'th detector, and let mean_ds2j and std_ds2j be the mean and standard deviation deduced for a large number of scan lines for detector j. Then, if on any one scan line ds2j > k* std_ds2j, then some kind of non-gaussian excursion may have occurred in the detector or the electronics. This is referred as a "pop" or "popcorn noise". The multiplier k has been tentatively set to 5 (TBD). The number of "pop's" observed during each 6 minute interval is counted and reported as pops/minute in the QA report. The data for the entire scan line from the detector where the "pop" was detected will be flagged as radiometrically bad. With k=5 there are about 60 of the 2378 AIRS detectors which show popping. These detectors have been flagged as bad. They are processed through level 1b.

4. Spectral Calibration

The AIRS Radiative Transfer Algorithm (AIRS-RTA) needs extremely accurate and stable spectral response functions (SRFs) for each AIRS channel to ensure that radiances calculated using the AIRS-RTA are within the AIRS noise level. Channel spectral centroids and widths are used (along with an appropriate shape model) to parameterize the SRFs. Requirements on the centroids and widths (taken directly from the FRD) state that the SRF centroids must be known at all times to within 1% of the SRF Full Width at Half Maximum (FWHM), the widths must be known to 1-3% of the FWHM (depending on spectral region), and the shapes of the SRFs have to be known to less than 0.1% of peak response in the wings for all scene conditions.

Determining the shape of these SRF's is a pre-launch calibration task and therefore is not part of the Level 1B algorithms. The of SRF shape and position uncertainty on the accuracy of the upwelling spectrum calculated by the forward algorithm is discussed in the L2 ATBD. Determining the spectral positions [centroids] of these SRF's is the Level-1B spectral calibration task.

The AIRS spectrometer has a spectral resolution $R = \lambda/\Delta\lambda$ nominally equal to 1200, where $\Delta\lambda$ is a detector's full width at half its maximum response (FWHM). The Functional Requirements Document (FRD) calls for a knowledge of detector centroid frequencies (for each array element) to within 1% of $\Delta\lambda$ at all times. These frequencies are not to vary by more than 5% over any 24 hour period. The FRD also demands knowledge of $\Delta\lambda$ no worse than 1%.

4.1 Conceptual Approach

AIRS in-orbit infrared spectral calibration is absolute, using identified features at known spectral locations in observed upwelling radiance spectra. It is based primarily on three components:

1) Focal plane detector assembly models;
2) A spectrometer grating model; and
3) Upwelling radiance spectra [both measured and modeled].

The focal plane detector assembly models specify the position of each AIRS infrared detector on the focal plane assembly, relative to the other detectors. A different focal plane detector assembly model is used for each of the three spectrometer thermostat set-points (149K, 155K, and 161K).

Three precision screws in the Actuated Mirror Assembly (AMA) can be turned in flight, finely repositioning the focusing mirror. The AMA will be moved only during the on-orbit instrument check-out to optimize the position of the dispersed entrance slit image on the detector arrays.

The spectrometer grating model specifies the relation between detector SRF centroids and detector physical positions (relative to the grating and the imaging optics). This is discussed at greater length in section 4.2.

The radiance spectra [both modeled and measured] provide "tie-points," allowing determination of the absolute position of the focal plane detector assembly. This is discussed at greater length in section 4.3.

The underlying assumption allowing this approach is that, for a given instrument condition (spectrometer temperature and optics alignment), the focal plane detector assembly, the relative positions of the entrance slits and relative positions of the dispersed images of the entrance slits on the focal plane remain invariant with temperature. This assumption has been born out by three types of test performed pre-launch:

A) Detector response centroids were measured before and after acoustic and vibration testing. Differences observed in detector SRF centroid (corresponding to 13% of $\Delta\lambda$) were consistent with a shift of the focal plane assembly relative to the spectrometer optics.
B) Detector response centroids were measured in both +1g and –1g environments (to estimate the magnitude of zero-g release effects). Differences observed in detector SRF centroids (corresponding to 3% of $\Delta\lambda$) were consistent with a shift of the focal plane assembly relative to the spectrometer optics.
C) Detector response centroids were measured repeatedly during an extended (24-hour) test simulating 14 day-night heating cycles. Again, differences observed in detector SRF centroids (this time corresponding to just 0.25% of $\Delta\lambda$) were consistent with a shift of the focal plane assembly relative to the spectrometer optics.

4.2 Spectrometer Model

In principle, the positions of the SRF centroids are given by the standard grating equation,

$$m * \lambda_i = d * (\sin(\alpha_i) + \sin(\beta_i)), \qquad \text{Eq. 4.1}$$

where m is the grating order, λi the wavelength of the i-th channel, d = 77.560 μm is the groove spacing of the grating, α_i is the angle of incidence and β_i is the angle of diffraction. Because of the

layout of the AIRS entrance slits, the incidence angle α takes on one of two values, 0.55278 or 0.56423 radians, depending on which detector array is being considered.

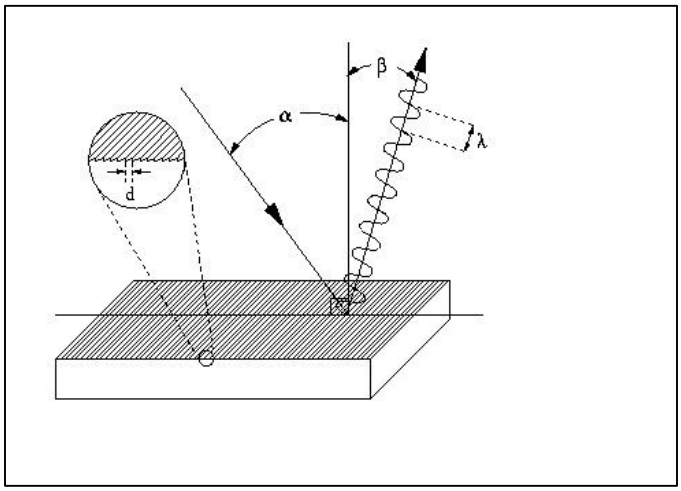

Figure 4-1 is a sketch of a simple grating spectrometer. The actual AIRS spectrometer is folded with a considerably more complicated layout, but the basic equation 4-1 applies. AIRS works in grating orders 3 (at the longest wavelengths) to 11 (at the shortest wavelengths). Through the use of two spectral bandpass filters for each detector array, one covering the spectrometer entrance slit, the other directly over each detector array, and geometric optics, each detector array is guaranteed to see radiation from only one grating order.

From the geometry of the AIRS optics, the diffraction angle β^k_i corresponding to the center of the i'th detector in the k'th array is given by

$$\beta^k_i = \text{atan}(y^k_i /(F_k + DF) \qquad \text{(Eq. 4.2)}$$

where F_k is the effective distance from the focusing mirror to the k'th detector array (very nearly equal to the focal length of the focusing mirror), and y^k_i is the distance (in the dispersed direction) from the optical axis to the center of the i'th detector in the k'th array. DF=0 for the pre-launch calibration. The very precise 50 μm spacing of AIRS detectors within an array then allows us to write

$$y^k_i = y^k_o + i*50\mu m + Dy_o \qquad \text{(Eq 4.3)}$$

Equation 4.3 is the focal plane model. This leaves us (for each "instrument temperature condition") just two parameters (per detector array), y^k_o and F_k , to determine the wavelength λi of each channel using Eq. 4.1. $Dy_o = 0$ for the pre-launch calibration. In order two allow a more accurate fit we introduced two additional parameter for each array, a_k and ν^κ , by defining the SRF centroid frequencies as

$$\nu_i = 1/\lambda i + a_k * (1/\lambda i - \nu^\kappa)^2 \qquad \text{(Eq. 4.4)}$$

The quantity ν^{κ} is the mean frequency of the k-th array. Equations 4.1 through 4.4. define the AIRS spectrometer calibration model. The model parameters a_k, y^k_o , Dy_o , λ^{κ} , DF and F_k are tabular entries in the Level 1B algorithm coefficient table. DF and Dy_o are zero initially, but are used in-orbit to fit the spectrometer model to the upwelling spectral radiance.

The determination of the SRF centroid model parameters was a pre-launch TVAC calibration activity. The results are summarized in Appendix 9. The model accuracy meets the required $0.01*\Delta\nu$ SRF centroid position knowledge requirement.

4.3 SRF Centroid Determination in Orbit

AIRS Level-1B software calculates and reports channel centroids once each granule (6 minutes, 135 scanlines). This is accomplished by comparing the positions of spectral features in the upwelling radiance against pre-calculated upwelling radiance features at known frequencies.

While the AIRS spectral calibration is extremely stable as a function of temperature, the focal plane detector assembly is likely to move (relative to the rest of the optics) due to launch vibrations. It will also move due to changes in the instrument's thermal environment. To allow for this motion, two small changes must be made to the components of the spectrometer model. The parameters DF and Dy_o allow for a focal length change and a optical axis shift common to all detectors. It is the determination of a change in in focal length DF and the shift of the optical axis relative to the center of the focal plane Dy_o that makes up the in-orbit spectral calibration task.

The in-orbit SRF centroid determination method can be summarized as: Determine the positions (on the detector array assembly) at which pronounced spectral features are located and Use this information to estimate Dy_o and DF in a least-squares sense.

The criteria for upwelling radiance feature selection, are described below.

4.3.1 Spectral Feature Fitting

The spectral features which have been selected are based on radiative transfer calculations with climatologically representative atmospheric conditions. Because radiative transfer in thermodynamically stable atmospheres is readily computable (good physics), and because absorption/emission line positions and strengths are well measured (good spectroscopy), the frequencies of the selected spectral features are also extremely well known.

The method used to determine the position of each spectral feature is as follow:

a) First, obtain an observed upwelling radiance spectrum. In principle, every AIRS spectrum could be used for wavelength calibration. In practice, only those four observations nearest nadir will be used which are reasonably cloud-free (as determined by a spectral contrast criterion, on a feature-by-feature basis). Such near-nadir, cloud free radiance spectra will be accumulated for six minutes (one granule of data) and averaged. The tremendous thermal stability of the AIRS instrument, as measured pre-launch, allows us to do this, even as the instrument crosses the terminator.
b) Then, using nominal values DF in the spectrometer model generate 11 trial frequencies sets using Dy_o = [-25, -20,… 0, 5, 10,..,25] μm.
c) Sample the pre-calculated radiance spectrum at these 11 frequency sets.
d) Calculate 11 correlation coefficient between each of the eleven sampled radiance spectra and the observed radiance spectrum, using the Pearson algorithm (Ref. 7).
e) Fit a parabola through the observed correlation coefficients, and determine value of Dy_o where the parabola peaks. (Note: Once the instrument has stabilized in orbit, 3 trial frequencies should be enough to determine the peak location.)

Pre-launch, the band center of each upwelling spectral feature (referred to as the "true" frequency of the feature) is converted to a position on the focal plane, using the nominal pre-launch spectrometer model. The 27 (TBD) feature shifts calculated above are added point-by-point to their pre-launch positions, producing 27 (TBD) observed feature positions.

These 27 (TBD) observed feature positions are then put through spectrometer model equations yielding 27 calculated frequencies. This process is repeated, optimizing the two parameters Dy_o and DF to minimize (in a least-squares sense) the difference between the calculated frequencies and the true feature frequencies. The downhill adaptive simplex algorithm "Amoeba" (Ref. 7) is used to find this minimum. With a global Dy_o and DF determined by the fit, a new frequency set is calculated using the spectrometer calibration equations. These frequencies are the "measured frequencies" reported by the level 1B software and archived with the data.

4.3.2 Spectral Feature Selection

Spectral features to which to fit observed radiance must satisfy a number of criteria:

1) Because these "tie-points" anchor the fit to the spectrometer grating model used for all detectors, the more features that are available to fit to, the better.
2) In order for the spectral calibration to apply equally well to all detector arrays, it is highly desirable for the spectral features to be distributed across the focal plane (evenly distributed, ideally).
3) For numerical fitting purposes, it is highly desirable to have the features be sharp (because translational fits are best done at places where radiance varies rapidly with frequency).

4) Most importantly, the calculated positions of the lines must not significantly change spectrally, under any anticipated climatological circumstances.

Table 4.1 lists the 34 spectral regions that have been identified as potential candidates for use as upwelling radiance features. A typical spectral region has 14 channels, but the number varies from eight to 26 channels. Regions 30, 31, and 32 are included in Figure 4-2.

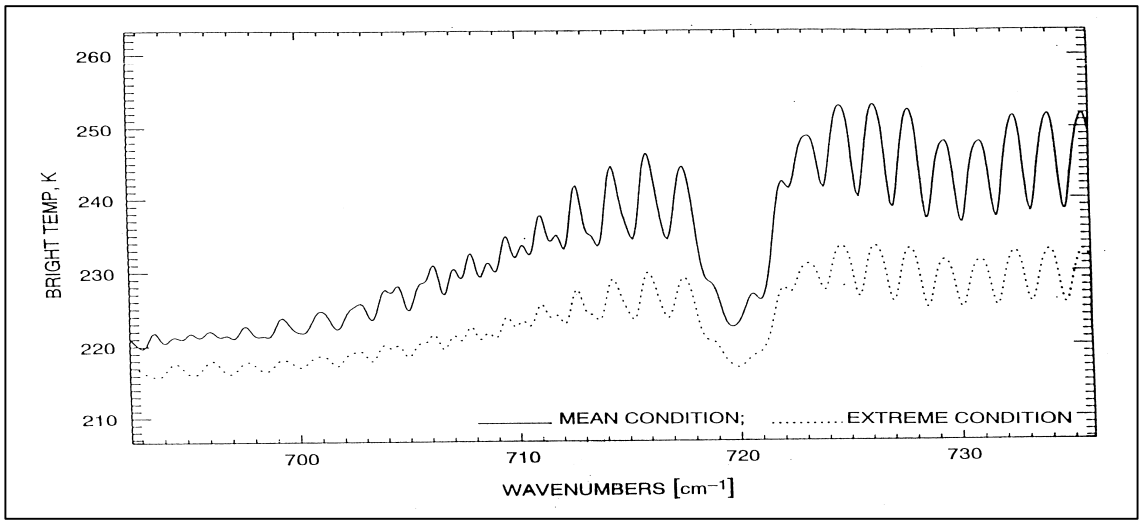

Figure 4.2. The spectrally resolved CO_2 spectral features in the 712 to 736 cm^{-1} region of the spectrum present an excellent region for spectral calibration.

The method used to determine suitability followed the on-orbit spectral calibration concept outlined in section 4.3.1:

a) The upwelling radiance for a US Standard temperature and moisture profile was calculated using the AIRS SRFs on a frequency grid corresponding to a nominal frequency model, and again for frequency grids corresponding to shifts in y_o by +/- 5, 10, 15, 20, and 25 microns.
b) Simulated "observed" AIRS spectra were then calculated (for each potential spectral feature) on these 11 frequency grids, for each of eight different extreme climatological conditions. The eight different climatologies were chosen to simulate anticipated variations in the upwelling radiance spectra.

Table 4.1. Candidate region evaluation for upwelling flux spectral calibration

region		LM#	LM#	array element			frequency [1/cm]	
#	mod	start	end	start	end		start	end
1	M1a	20	27	21	28	8	2642.94	2635.35
2		34	46	35	47	13	2627.81	2614.97
3		48	56	49	57	9	2612.89	2604.37
4		95	108	96	109	14	2563.85	2550.63
5	M1b	187	200	70	83	14	2355.09	2342.81
6	M2a	256	264	9	17	9	2560.46	2551.53
7		340	356	93	109	17	2469.66	2453.08
8	M2b	461	473	98	110	13	2229.3	2218.02
9	M3	593	617	80	104	25	1397.51	1384.3
10	M4a	709	721	4	16	13	1611.43	1602.64
11		765	781	60	76	17	1571.19	1560.73
12	M4b	820	833	11	24	14	1520.19	1511.67
13		868	893	59	84	26	1489.22	1473.58
14	M4c	944	956	29	41	13	1321.81	1314.7
15		976	984	61	69	9	1303.02	1298.41
16	M4d	1035	1044	26	35	10	1258.74	1253.88
17	M5	1142	1150	27	35	9	1122.45	1118.19
18		1159	1174	44	59	16	1113.44	1105.61
19		1178	1189	63	74	12	1103.53	1097.88
20	M6	1277	1290	3	16	14	1045.11	1039.07
21		1299	1311	25	37	13	1034.94	1029.47
22	M7	1497	1524	56	83	28	952.3	941.94
23		1566	1580	125	139	15	926.26	921.15
24	M8	1648	1661	40	53	14	890.29	885.92
25		1701	1710	93	102	10	872.77	869.87
26	M9	1797	1805	28	36	9	841.4	838.21
27		1828	1840	59	71	13	829.18	824.16
28		1914	1932	145	163	19	797.01	790.58
29	M10	2029	2047	93	111	19	751.02	745.88
30		2066	2090	130	154	25	739.32	731.91
31	M11	2108	2125	5	22	18	727.13	722.04
32		2141	2159	38	56	19	717.31	712.06
33	M12	2258	2278	11	31	21	679.27	674.07
34		2346	2366	99	119	21	657.01	652.16
typical number of detectors per region =						**14**		
				minimum=		**8**		

c) The locations at which the correlation between the "observed" and the pre-calculated spectrum peaked (and the resulting correlation coefficients) were determined, for each spectral feature, for each climatology.
d) Statistics were calculated over the eight climatologies, providing the mean and standard deviation for the observed shifts and correlation coefficients, on a feature-by-feature basis.

Table 4-2 shows the results. The suitability flag was determined by requiring the following:

1) A mean shift of less than 1.3 microns (this is equivalent to 1.3% of the SRF FWHM)
2) A standard deviation of the shift of less than 2.6 microns, and
3) A peak correlation coefficient larger than 0.98.

Based on these criteria, 27 of the 35 candidate regions are acceptable. The spectral features were located with a mean error of 0.05 microns. This corresponds to only 0.05% of $\Delta\nu$, the SRF FWHM. All arrays except M1b and M4d contain at least one acceptable spectral feature.

This test is actually a worst case test, since extreme spectra were compared to the US standard profile spectra. The AIRS level 1b software uses the same eight climatologies, but applies it at the location appropriate to the climatology. The mismatch between the calculated spectrum and the observed spectrum can thus be made arbitrarily small by choosing enough climatology cases.

Table 4.2. US Standard compared to 8 climatologies (without polar winter)

region		shift(um)		1.3	2nd deriv(x1000)		corr.coeff		0.98	2.6	all region summary
#	mod	mean	sigma		mean	sigma	mean	sigma			good=0
1	M1a	-0.60	1.08	0	0.69	0.01	0.996	0.003	0	0	0
2		1.19	1.04	0	0.18	0.02	0.997	0.003	0	0	0
3		-0.57	0.37	0	0.30	0.01	0.995	0.005	0	0	0
4		-9.41	10.96	1	0.05	0.01	0.993	0.009	0	1	1
5	M1b	-0.73	1.14	0	0.17	0.00	1.000	0.000	0	0	0
6	M2a	-1.30	1.43	0	0.12	0.01	0.999	0.001	0	0	0
7		0.08	2.48	0	0.02	0.00	1.000	0.001	0	0	0
8	M2b	-1.86	2.63	1	0.10	0.00	1.000	0.000	0	1	1
9	M3	-0.02	0.05	0	0.12	0.00	1.000	0.000	0	0	0
10	M4a	-0.21	0.12	0	0.58	0.00	1.000	0.000	0	0	0
11		-0.05	0.26	0	0.25	0.00	0.999	0.001	0	0	0
12	M4b	0.08	0.37	0	0.32	0.00	0.999	0.001	0	0	0
13		0.17	0.17	0	0.15	0.00	1.000	0.000	0	0	0
14	M4c	-0.30	0.99	0	0.26	0.02	0.998	0.004	0	0	0
15		-0.45	0.06	0	0.32	0.00	1.000	0.000	0	0	0
16	M4d	-0.44	6.55	0	0.46	0.08	0.986	0.009	0	1	1
17	M5	-0.90	1.31	0	0.54	0.05	0.988	0.019	0	0	0
18		0.05	1.33	0	0.51	0.02	0.995	0.006	0	0	0
19		-0.07	4.51	0	0.52	0.04	0.993	0.010	0	1	1
20	M6	0.23	0.39	0	0.06	0.00	1.000	0.000	0	0	0
21		1.60	1.84	1	0.52	0.04	0.988	0.019	0	0	1
22	M7	0.91	4.00	0	0.32	0.05	0.980	0.028	0	1	1
23		-1.03	1.28	0	0.35	0.02	0.987	0.013	0	0	0
24	M8	0.13	0.15	0	0.34	0.00	0.995	0.005	0	0	0
25		-0.04	0.13	0	0.31	0.01	0.999	0.001	0	0	0
26	M9	1.17	1.55	0	0.48	0.03	0.997	0.002	0	0	0
27		-0.89	1.56	0	0.52	0.02	0.993	0.008	0	0	0
28		0.60	0.86	0	0.58	0.01	0.976	0.021	1	0	1
29	M10	-0.09	0.31	0	0.55	0.00	1.000	0.000	0	0	0
30		0.04	0.20	0	0.65	0.00	1.000	0.000	0	0	0
31	M11	-0.04	0.34	0	0.55	0.01	0.999	0.001	0	0	0
32		-0.02	1.02	0	0.51	0.00	0.999	0.001	0	0	0
33	M12	0.02	0.25	0	0.42	0.01	0.998	0.001	0	0	0
34		-0.14	1.07	0	0.48	0.01	0.997	0.003	0	0	0
		-0.05	**microns**								**27**
all array median position error								**total number of good regions**			

4.4 Spectral Calibration Error Estimation

The uncertainty in the SRF centroid position determined by the spectral calibration algorithm has four main components:

1. The uncertainty in the spectrometer calibration model (based on pre-launch calibration), $\delta\nu_1$.
2. The uncertainty in the determination of y_o and F_o in orbit based on the finite number of spectral tie-points obtained from the upwelling spectra, $\delta\nu_2$.
3. the mismatch between the pre-calculated climatology spectra and the actual upwelling radiance, $\delta\nu_3$.

The mismatch between the calculated climatology spectrum and the observed spectrum can be made arbitrarily small by choosing enough climatology cases. The magnitudes of the rss uncertainties differ from array to array, but they are dominated by the uncertainty of the spectrometer calibration plane model, $\delta\nu_1$ (Appendix 4. Figure A.4.1), which is less than 1% of $\delta\nu$.

Accurate knowledge of the SRF FWHM and the SRF wing response is critical for the accurate calculation of the transmittance function in the Radiative Transfer Algorithm (RTA). Direct determination of the shape of the SRF in orbit is not possible and is not part of the Level-1B calibration algorithm. Errors in the knowledge of the SRF width and/or wing response will mimic radiometric errors, which under some conditions of high spectral contrast may become the dominant radiometric error. The routine validation program monitors radiometric biases in all channels with an accuracy of 0.1K. Changes in the SRF shape would show up as gain errors with a pronounced spectral dependence, which mimics the spectral contrast of the upwelling radiance. Details of the routine bias evaluation are given in Appendix 6.

5. Spatial Calibration

The AIRS infrared data, with a 1.1 degree effective FOV, will be analyzed simultaneously with microwave data from the AMSU (3.3 degree beam), and the HSB (1.1 degree beam). Knowledge of AIRS FOV location on the ground has to be within a 255 arc second half cone angle. The requirement is easily met by the spacecraft knowledge of the pointing vector within 12.2 arcsec (1 sigma). The selection of several AIRS FOV's within the AMSU FOV is thus based on data from instrument integration. Details of the selection of AIRS FOV clusters located within the AMSU FOV are discussed in the level 2 ATBD. No AIRS infrared pixel interpolation is required or included in the level 1b algorithm.

5.1. Infrared Boresight Validation

The AIRS infrared boresight relative to the scan mirror axis was determined during TVAC. The level 1a software combines the scan mirror shaft encoder data and spacecraft telemetry to determine the infrared boresight. Validation of the AIRS infrared boresight at the team leader facility is planned to facilitate cross-comparisons between AIRS and other instruments on the EOS PM spacecraft. This algorithm is part of the in-orbit validation software, and as such not part of the level 1b software. A description of the concept is included in the following because of general interest.

The algorithm will make use of the statistics of crossings of high contrast scenes (e.g. transitions from land to ocean) to determine a longitude and latitude offset angle between the apparent boundary location and the true boundary location. If the temperature contrast between ocean and land is ΔT_{ol} , the spectrometer noise equivalent temperature per footprint is *NEDT*, the angular footprint diameter is Φ, and the average angle between the cross-track scan and the coastline intersection is α, then the statistical accuracy of the cross-track position accuracy determination from n crossings is

$$\frac{\Delta\Phi(n)}{\Phi} = \frac{NE\Delta T \cos(a)}{\Delta T_{ol}\sqrt{n}} \qquad \text{Eq. 5-1}$$

For typical values of α=45 degree, NEΔT=0.2 K and ΔT_{ol}=10 K, we obtain

$$\frac{\Delta\Phi(n)}{\Phi} = \frac{0.03}{\sqrt{n}}.$$

Cross-track boresight determination (as the difference between the infrared boresight observed and the geometric boresight calculated) to within 1% of the AIRS field-of-view is achievable with 10 coastline crossings. In practice, a single orbital pass along Baja California produces about 200 coastal crossings suitable for verification of the infrared boresight. This scheme has been used successfully for ERBE and for CERES on the TRMM and EOS Terra.

6. References

1. Development and Test of the Atmospheric Infrared Sounder (AIRS) for the NASA Earth Observing System (EOS), Paul Morse, Jerry Bates, Christopher Miller, Moustafa Chahine, Fred O'Callaghan, H. H. Aumann and Avi Karnik SPIE 3870-53, 1999.

2. AIRS Functional Requirements Document, JPL Internal Document D- 8236, Rev. 1., Oct. 1992.

3. AIRS Calibration Plan, JPL D-16821, 14 November 1997. http://eospso.gsfc.nasa.gov/calibration/plans.

4. AIRS Team Science Validation Plan, Core Products, JPL D-16822, Version 2.1 15 December 1999 ftp://eospso.gsfc.nasa.gov/sterling/Validation/AIRSplan.pdf

5. World Meteorological Organization, "The World Weather Watch Programme 1988-1997", WMO-No. 691 (1987)

6. AIRS Algorithm Theoretical Basis Document, AIRS Team Unified Retrieval for Core Products (Level 2 ATBD) JPL D-17006, Version 2.1 15 December 1999 http://eospso.gsfc.nasa.gov/atbd/airstables.html

7. Press, W. et al., 1992, Numerical Recipes in Fortran 77: The Art of Scientific Computing, (New York: Cambridge).

8. "AIRS instrument polarization response: measurement methodology", G. Gigioli and T. Pagano, SPIE 3759-30, July 1999

9. AIRS Scan-mirror polarization measurements (1998) Dr. Mike McDonald, MIT Lincoln Lab, personal communication.

10. Bruker Instruments Model IFS-66V

11. US Guide to the Expression of Uncertainty in Measurement, NCSL, ANSI/NCSL Z540-2-1997.

Appendix 1. Frequently Asked Questions (FAQ)

In the following we answer "Frequently Asked Questions" regarding the AIRS Infrared Spectrometer: Radiometric Calibration, Spectral Calibration and in-orbit Calibration Validation. This includes all questions raised by reviewers of the level 1b IR ATBD in February 1997 and March 2000 and some additional ones posed by members of the user community.

1. Questions about the radiometric calibration

How will the degradation of the OBC emissivity be monitored?

See AIRS level 1b ATBD Appendix 6 discussion of routine bias monitoring. A change in the OBC emissivity will cause a decrease in the apparent gain of the detectors. Assume that the actual gain of the detectors actually remained unchanged. This change in the gain will be detected by the routine QA (monitoring the normalized gain). The level 1b software will compensate for the apparent decrease in gain by increasing the signal from the scene. This will show up in the bias equation: Coefficient *b* will be less than one on all or some detectors. A gain error of 0.1K level can be detected in the time history plots. Plot *b* as function of wavelengths. Any spectral signature or array dependence will help to diagnose what the problem is and what corrective actions are needed.

Is the LABB and OBC traceable to NIST?

Yes. The Large Area Blackbody output is NIST traceability based on contact thermometry using PRT's and its state of the art design. This is discussed in AIRS level 1b ATBD section 2.2. and Appendix A3.2. In the AIRS temperature range between 200 and 350K and for the AIRS accuracy requirement reliance on contact thermometry and good design practice are adequate.

How is Cold Space View (CSV) contamination by horizon proximity and moon addressed?

The location of the CSV relative to nadir and the Earth horizon is discussed in AIRS level 1b ATBD Section 2.2. Section 3.1.2 discusses the space view selection algorithm. The validity of this algorithm has to be confirmed in orbit. The CSV at 64.4 degree may well be permanently unusable. The strategy of multiple space view with selection optimization in orbit is also used on AMSU-A and AMSU-B.

How does polarization effect the calibration? Is the difference between the calculated and the measured polarization understood?

The source and the effect of polarization in the AIRS calibration is discussed in AIRS level 1b ATBD Section 3, with further details in Appendix 3. Polarization is very difficult to calculate for a coarse grating used by AIRS. The agreement is surprisingly good most places. The directly measured polarization is used in all cases for the $p_r p_t$ correction term in the AIRS radiometric calibration equation.

How is detector striping (non uniform response to a uniform scene) corrected?

In the AIRS spectrometer all detectors (on linear arrays) share the same field-of-view, i.e. for radiometric calibration purposes AIRS acts like 2378 single channel spectrometers. The radiometric calibration process normalizes the gain of all detectors to a common (OBC) blackbody. Detector striping is a common problem with spatial (linear and area) array detectors.

When adjusting each detector gain (accounting for a different spectral interval) to the 308K blackbody, will the correction work for a cold scene (such as clouds) as well as for the warm scene?

This is discussed in AIRS level 1b ATBD Section 3 and Appendix 3. Correction terms have been developed based on the measured response from the LABB stabilized at 205K to 360K in steps of 15K to "adjust each detector" to give the correct output for cold and warm scenes. The accuracy of these correction terms has been directly demonstrated. This is discussed in Section 3.

The presence of "popcorn noise" may degrade the radiometric calibration. How is this handled by the Level 1B software?

The popcorn detection algorithm is described in AIRS level 1b ATBD Section 3.3. Pop-corn type noise has been observed in only about 60 of the 2378 AIRS channels. These channels will not be used for direct assimilation or retrievals.

If a pop-event is detected, the entire scan line for this detector is flagged as "radiometric calibration out of spec". Since the pop frequency is typically one pop in 500 seconds or less, the probability of two pop's to occur one scan line or between space views (separated by 22 msec) is

extremely small. Data users who can not avoid using a channel which pops need to familiarize themselves with the radiometric validity flags generated routinely by the level 1b software.

Was the scan mirror non-uniformity calibrated in TVAC tests before launch?

Yes. This is discussed in the AIRS level 1b ATBD section 3.4. The effect is sufficiently small to be negligible and still meet the AIRS absolute calibration requirements. Measurements during TVAC as function of scan angle have not detected unusual scan angle dependence of the calibration not explained by the $p_r p_t$ polarization effect.

Can changes in the scan mirror emissivity on-orbit for those positions on the mirror used to view the Earth be detected?

See AIRS level 1b ATBD Appendix 6 discussion of routine bias monitoring of the Earth scene. A change in the scan mirror emissivity for both Earth view and OBC positions will results in a decrease in the detector gain, due to reflection = (1-emissivity). Since the scan mirror is cold, the emitted radiance change is very small. A decrease in reflection is exactly compensated by the level 1b gain calibration. The gain decrease will show up as a trend in the time history plot. A spectral plot of the normalized gain/pre_launch_gain will be aid the diagnostic of the type and spatial distribution of the emissivity change. Given the location of the scan mirror the likelihood of non-uniform emissivity degradation (scene areas only) is very small.

The AIRS scan mirror emissivity may change in orbit due to contamination. Could the scan mirror emissivity be calculated using the cold-space-view experiment proposed by the MODIS and CERES teams?

1. The AIRS radiometric calibration has no sensitivity to the mean value of the scan mirror emissivity. A scan angle dependent variation in the emissivity would have an effect. This is discussed in AIRS level 1b ATBD Section 3. Under worst case assumptions the effect is negligible for AIRS instrument conditions and calibration requirements.

2. It would be desirable to measure the emissivity of the scan mirror at all scan angles for all wavelengths directly in-orbit and include it as another scan angle dependent correction term. However, the proposed experiment does not provide for AIRS the information required to calculate the emissivity as function of scan angle.

CERES and MODIS have proposed a cold-space scan maneuver with the Aqua satellite to measure radiometric parameters, including scan mirror properties. In the proposed experiment

the spacecraft nadir position is rotated 180 degrees. The AIRS scan mirror could then scan cold space in 90 steps from -49 to +49 degrees, plus the four regular space views. For the AIRS scan mirror scene-view, space view, and OBC view configuration (AIRS level 1b ATBD, figure A3.7) this experiment has two significant shortcomings:

1) the emissivity of the scan mirror in the OBC view position is not measured.
2) In order to make measurements at or below the NEN level many minutes of scanning are required. The electronics and background drift due to temperature changes will have to be cancelled through the use of the normal space views. Thus, only the difference between the scan mirror emissivity in the scene views and the cold space view can be measured.

The routine QA monitoring using Level 1B generated metrics will allow detection and identification of potential scan mirror contaminants:

1) the statistics of the difference between adjacent space views is a measure of scan mirror emissivity non-uniformity on a 40 degree scan mirror sector. A change in the difference would suggest a change in the optical properties.
2) Plotting the normalized gain as function of frequency was used during TVAC to detect contamination of the mirror and identify it as water ice.

Have possible changes in emissivity over the lifetime of AIRS be modeled?

Yes. This is discussed in AIRS level 1b ATBD Appendix 3.4, figure A3.8.
The assumptions about emissivity degradations in space are very exposure sensitive. The AIRS scan mirror is located in a fairly protected area and is always latched in its launch-protected position (looking into the OBC) during space maneuvers requiring rocket thrusters. The data suggest a bias of 0.05K to 0.1K between start of mission and after five years in orbit. Bias at this level is detectable, as discussed in Appendix 6.

2. Questions about the spectral calibration.

Why does AIRS use Earth scene radiances for spectral calibration rather than a well-characterized calibration source.

For the AIRS accuracy requirement the upwelling spectral radiance is the one obvious and only reliable spectral calibration source. AIRS level 1b ATBD Table 4.2. shows the location of the selected spectral features.

What is the error due to the use of calculated radiances (which are imperfect) for spectral calibration?

Spectral features due to resolved isolated lines do not shift, but some spectral features which are only partially resolved will show an apparent shift. Spectral features which show excessive sensitivity have been identified in AIRS level 1b ATBD Table 4.2. and have been rejected. Spectroscopic error at levels relevant to AIRS are exclusively line strength or line shape errors, not line position errors.

How does contamination by clouds and thin cirrus affect "clear" scene spectral calibration?

No effect. This is discussed in AIRS level 1b ATBD section 4.1. and Table 4.2. Clouds, including cirrus clouds, will have little effect on the spectral calibration, since they lack the pronounced spectral signatures of the atmospheric gases over the narrow spectral range used in the frequency calibration.

Will the OBS be used in-orbit?

No. The OBS, described in AIRS level 1b ATBD Section 2.2, allows estimation of focal plane position with an accuracy of about 1 micron, i.e. the equivalent of 1% of the SRF width. The OBS does not have enough spectral features distributed over the AIRS spectral range to be suitable for spectral calibration. The OBC was very useful for pre-launch testing, where the use of the Bruker interferometer was impractical, and for system testing in TVAC at TRW, where there are no other spectral reference sources. In orbit the AIRS spectral calibration depends entirely on the location of features in the upwelling spectral radiance, as described in Section 4.

How often will the AMA be used in-orbit for spectral calibration*?*

The AMA is used to optimize the position of the images of the entrance slits on the detector arrays (effectively the exit slit of the spectrometer) with a motion in the cross-dispersed direction. The AMA, discussed in AIRS level 1b ATBD Section 2.1, allows motion in the dispersed, cross-dispersed and radial (focus) axis. There is no plan to move the AMA in the dispersed direction in orbit.

Do changes in the grating temperature effect the spectral calibration? How does the grating constant vary with temperature? Can the required thermal stability be achieved?

This is discussed in AIRS level 1b ATBD Section 2.1. The effect of spectrometer temperature on the spectral calibration was measured in TVAC. A spectrometer temperature change causes an apparent shift in the focal plane position of 2.7 micron/degree K. Since the SRF width is equivalent to 100 microns, this corresponds to a shift of 2.7% of the SRF width per degree K temperature change. The effect is due to the expansion coefficient of the Aluminum of the grating, i.e. the grating constant changes.

The AIRS spectrometer has a time constant of 20 hours and the temperature is regulated at a set point to within 30mK. The spectral stability was tested under simulated orbital conditions. During the simulation of 24 hours "in orbit" the observed amplitude of the apparent focal plane motion was +/- 0.3 microns. A shift of less than 0.5 micron, corresponding to 0.5% of the SRF width, is practically negligible.

After thermal equilibrium is achieved (estimated to take about two week, based on the experience in the ATCF), the spectral calibration of AIRS is expected to be extremely stable. Any spectral features in the SRF, known or unknown, are essentially frozen in. The activities planned under routine spectral calibration are thus more in the nature of spectral stability calibration monitoring.

Can in-orbit changes in the SRF characteristic be detected? What can be done about them?

1. This question is addressed in AIRS level 1b ATBD A.7.2. Would it be detectable? Yes. Is it likely to happen? No, as long as the spectrometer is maintained at its set point temperature the SRF shape is frozen into the design.
2. How would we tell? A change of 1% in the SRF effective width can cause a signal shift of the order of 0.2K in high spectral contrast locations. Based on data simulation using many profiles 90% of this shift is a bias, 10% results in increased standard deviation (noise). If the SRF characteristics were to change, but the forward algorithm is not changed to account for

the new SRF, then the routine bias monitoring program (Appendix 6.), which can detect a bias of as little as 0.1K, will flag it.

3. What will be done about it depends on the user:
   a) Operational assimilation: The operational direct assimilation software automatically applies the bias correction and proceeds with the assimilation. This removes the bias, but not any additional noise introduced by the change. There is little impact on the operational forecast system performance, as long as these change occur slowly (on a months timescale). Stability on this timescale is implicit in the AIRS thermal design.
   b) Research users: The AIRS level 1b QA metrics are use to monitor a large number of parameters of the spectrometer. If a new bias is detected: Is the SRF centroid calibration normal? Was a change in plate scale (focal length change) noted? Is it happening on all channels or only at some wavelength? Are there changes in one of the six spectrometer temperature sensors? Is the gain calibration? Are there spectral features in the normalized gain spectrum? With the AIRS spectrometer design the shapes of the SRF and their positions relative to each other are highly correlated. Plot of the *a* and *b* bias equation coefficients will show a very high correlation with the upwelling radiance spectrum for those arrays which are involved. The TLSCF will attempt to deduce from various indicators where the bias is coming from and how to eliminate it at its root, rather than to simply subtract it out.

3. Questions about Level 1b Validation

What if any feedback is there between bias monitoring and level 1b software?

a) Operational users: The current operational direct assimilation software at NCEP and ECMWF automatically applies all bias corrections. This software is thus inherently using a type of vicarious calibration.
b) Research users: Any significant bias or change in bias detected by the bias monitoring software will be analyzed to separate instrumental effects from radiative transfer, or true atmospheric effects (such as an increase in the CO_2 amount) by using the high spectral information content of AIRS, including spectral characteristics of the terms of the bias equation (AIRS level 1b ATBD Appendix 6 and Appendix 7).

Is SST used for vicarious calibration?

No. Given the accurate radiometric characterization and stability of AIRS demonstrated during TVAC testing, vicarious calibration is not compatible with a NIST traceable calibration and the NASA climate research objectives.

Vicarious validation of the IR channels will be used for routine processing, i.e. the global forecast and data from highly instrumented surface sites will be used to compare (calculated-observed) for all channels (Appendix 6 and Appendix 7, copied from the AIRS Validation Plan). Reynolds SST and floating buoys will be used in the initial level 1b validation process and routine level 1b QA. This monitoring effort includes scatter diagrams of the deviations (residuals) of the observed temperature from the ground-truth temperature as function of temperature (270K to about 310K) and as function of scan angle.

The process of vicarious validation differs from the process of vicarious calibration: Vicarious validation minimizes the residuals between measured radiances and radiances calculated based on ground-truth data by analyzing the root of the discrepancy and fixing the “error” at the root. This not only eliminates a bias under a specific condition, e.g. at 270K surface temperature, but it decreases the bias at other conditions, e.g. much colder temperatures which can not be readily validated via ground truth. If spectral patterns in the residuals suggests a problem with the level 1b or level 2 software, appropriate corrections will be made in the software. This procedure eliminates bias and decreases the residual scatter. Vicarious calibration empirically minimizes the residuals between calculated and observed. This only eliminates a bias at a specific condition (perhaps only at one validation site).

Appendix 2. Dictionary of Abbreviations

ADC	Analog to Digital converter
AIRS	Atmospheric Infrared Sounder
AMSU	Advanced Microwave Sounding Unit
ATBD	Algorithm Theoretical Basis Document
ATCF	AIRS Test and Calibration Facility (TVAC)
CSV	Cold Space View
DCR	DC Restore (of the electronics)
DN	Data Number
DOD	Department of Defense (US)
ECMWF	European Center for Medium range Forecasting
EM	Engineering Model
EOS	Earth Observing System
FOV	Field of View (projected on the ground pertaining to one dwell time)
FM	Flight Model
FRD	Functional Requirements Document
GSFC	Goddard Space Flight Center
HgCdTe	Mercury-Cadmium Telluride
HIRS	High Resolution Infrared Sounder
HSB	Humidity Sounder Brazil
IFOV	Instantaneous Field of View. Smaller or equal to the FOV.

IR	Infrared
JPL	Jet Propulsion Laboratory
MODIS	Moderate Resolution Imaging System (on EOS-Am and PM)
MSU	Microwave Sounding Unit
NASA	National Aeronautics and Space Administration
NEDT	Noise Equivalent Delta Temperature
NEN	Noise Equivalent Radiance
NIR	Near Infrared (between 1 and 3 microns)
NIST	National Institute of Standards
NOAA	National Oceanic and Atmospheric Administration
NWS	National Weather Service
OBC	On-Board Blackbody Calibrator
OBS	On-Board Spectral reference source
PC	Photoconductive Detector
PFM	Proto Flight Model
PRT	Platinum Resistance Thermometer
PV	Photo Voltaic Detector
QA	Data Quality Assessment
SRF	Spectral Response Function
TBD	To Be Determined
TVAC	Thermal Vacuum Chamber
VIS	Visible wavelength

Appendix 3. Radiometric calibration

The radiometric calibration consists of two major steps: 1. The determination of the radiometric transfer coefficients using a NIST traceable black body external to the instrument and 2. The transfer of the LABB calibration to the On-Board Calibrator (OBC).

A3. Radiometric Calibration Coefficients and Uncertainties

A3.1 Calibration Coefficients

The AIRS calibration equation defines the input radiance, *N*, as function of the difference between the signal from the raw scene view signal, *dn*, and the raw signal from the cold space view, dn_{sv} ,

$$N_{sc,i,j} = \frac{a_o(q_j) + a_{1,i}(dn_{i,j} - dn_{sv,i}) + a_2(dn_{i,j} - dn_{sv,i})^2}{1 + p_r p_t \cos[2(q_j - d)]} \qquad \text{Eq 3-1}$$

The three radiometric transfer coefficients a_o, a_1 and a_2 of the calibration equation were evaluated using the LABB. Data were acquired from the AIRS while viewing the LABB as it was stepped through several temperature levels from 205K to 310.

Step 1. Approximate $p_r p_t$. The set of data $\{N_{LABB}$, dn-$dn_{sv}\}$ were fit to a second order polynomial to obtain a_o, a_1 and a_2. We then assume that the a_o term is entirely due to polarization effects because the intercept should be zero since we are subtracting the signal while viewing space from every sample. According to equation 3-6

$$a_o(q_j) = N_m p_r p_t \left[\cos 2(q_j - d) + \cos 2d\right]$$

$$p_r p_t = a_o / 2N_m$$

The resulting $p_r p_t$ is presented in section A.3.3 with the other techniques for obtaining this parameter.

Step 2. Fit to obtain a_1 and a_2. Now that we have a good estimate of $p_r p_t$ we can fit the data set $\{N_{LABB}(1+p_r p_t \cos(2\theta-\delta)) - a_o)$, dn$\}$ to a second order polynomial to obtain a_1 and a_2. The a_1 is the gain, but this will be updated in orbit with the OBC blackbody. The a_2 are the final flight

values. Figure A3.1 shows the nonlinearity for AIRS expressed as a fractional signal contribution at 280K; i.e.

$$\text{Nonlinearity} = a_2\, dn^2 / (a_1\, dn + a_o)$$

This data has undergone a 5 point smooth by channel to minimize noise in the a_2 term. We see less than 1.5% nonlinearity across all channels and less than 0.5% for most.

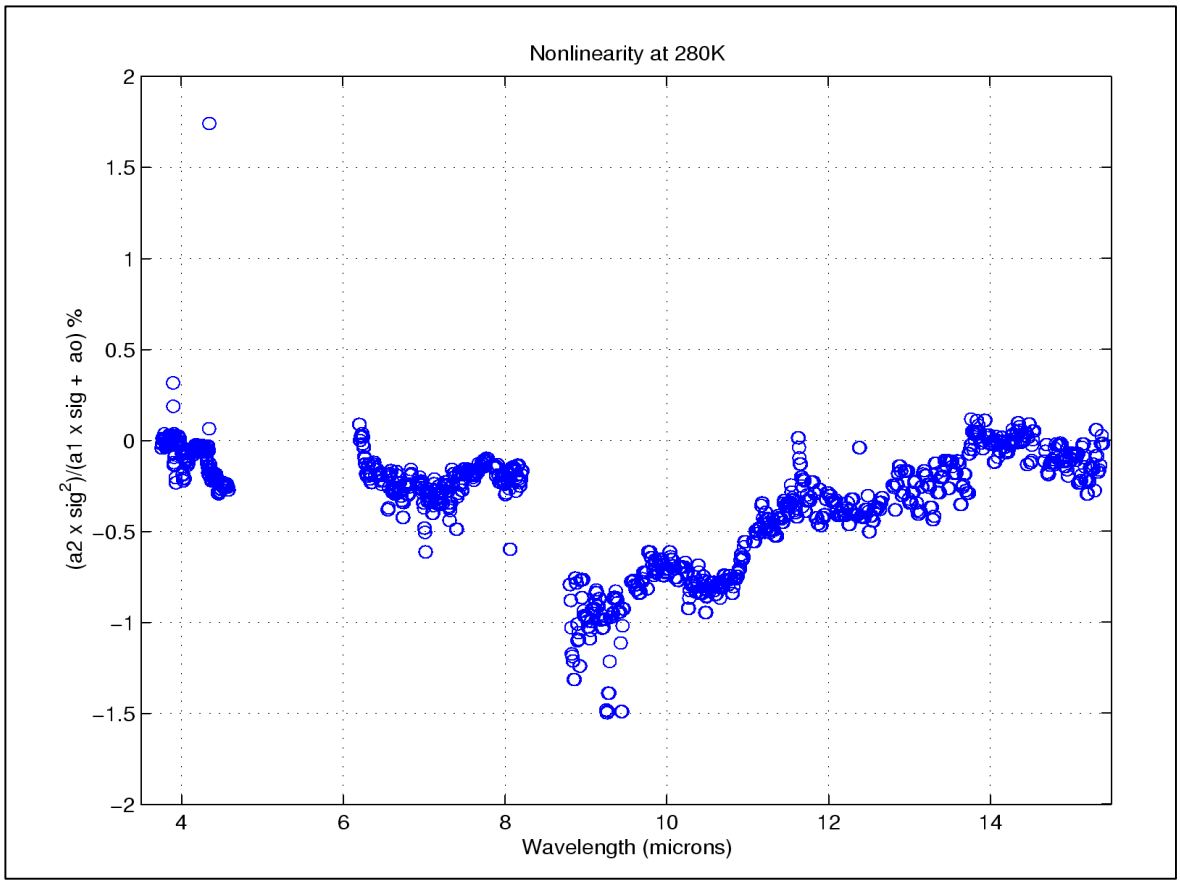

Figure A3.1. Nonlinearity for AIRS is less than 1.5% for all channels

Step 3. Uncertainty Estimate, ? a_2 : We determine the uncertainty in a_o through the uncertainty in $p_r p_t$. This is discussed in section 3.3. The uncertainty in a_1 is replaced by the OBC temperature uncertainty and the gain correction term discussed in section A3.2. The uncertainty in a_2 is determined by taking a running 5 point variance on all the AIRS channels of the a_2. This gives us an estimate of the variance in the a_2 term.

A3.2 OBC Gain Correction Term

A gain correction term allows us to correct the apparent radiance of the internal OBC BB to match the external LABB. We obtain the correction term by evaluating the OBC radiance at the OBC temperature using the coefficients obtained during LABB linearity testing; we call this the "derived" radiance. The gain correction term is the ratio of the derived radiance to that determined by the OBC temperature sensors.

$$e_{OBC} = \frac{\dfrac{a_o(q_{OBC}) + a_{1,i}(dn_{i,j} - dn_{sv,i}) + a_2(dn_{i,j} - dn_{sv,i})^2}{1 + p_r p_t \cos[2(q_{OBC} - d)]}}{P_{OBC}\left(T_{OBC\_meas} + 0.3K\right)}$$

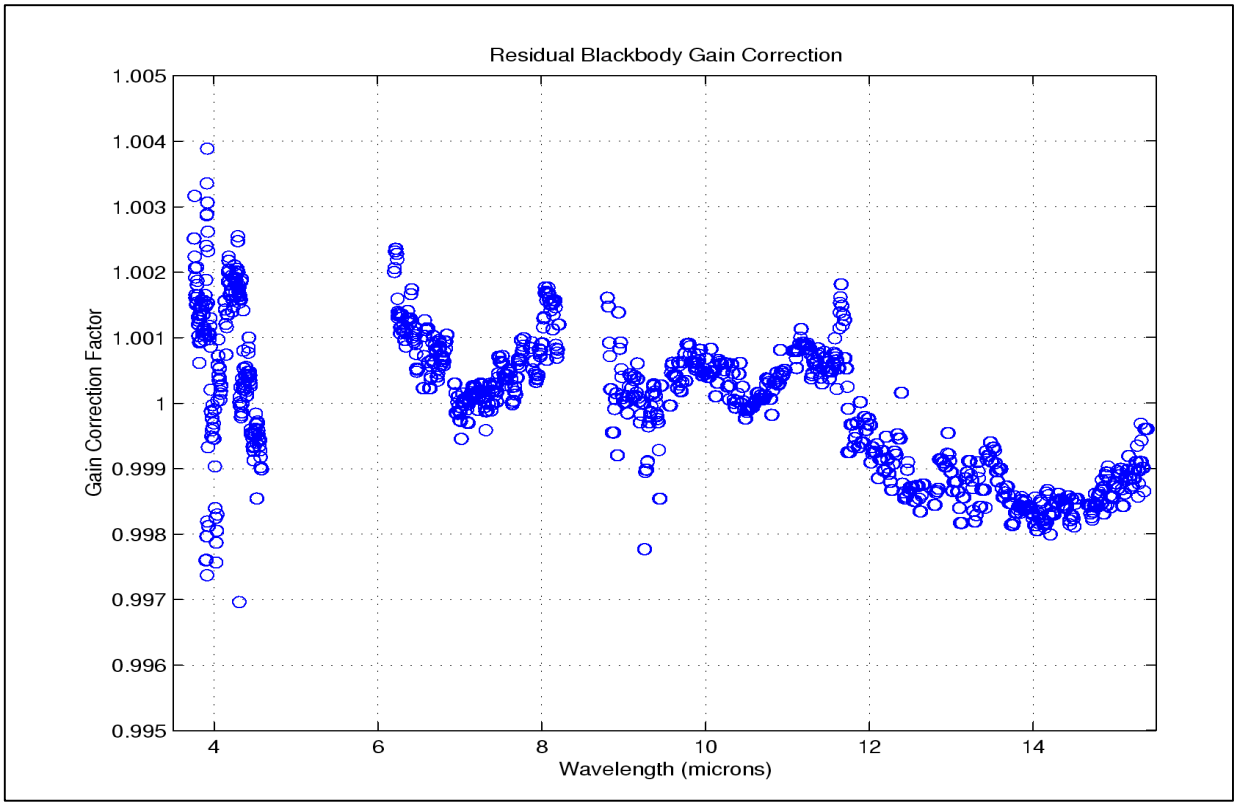

Figure A3.2. The OBC gain correction term, the ratio of the LABB signal to the AIRS OBC BB signal at the OBC temperature, is within 0.002 of unity. The terms "OBC gain correction" and "OBC effective emissivity" are equivalent.

We have corrected the "as measured" OBC temperature to the "effective" OBC temperature by adding a 0.3K offset as an additional calibration term (see Eq. 3.4) prior to applying the gain correction. This temperature offset is within the expected uncertainty of the combined OBC temperature sensors calibration, the electronic conversion of the sensor signal to digital number, and the conversion from dn to engineering units (Kelvin). Figure A3.2 shows the gain correction term for AIRS. We see corrections of less than ±0.2% are required across all channels. We do not understand at this time the nature of these very small correction terms, but speculate that they are due to a small, spatial temperature inhomogeneity in the OBC. The uncertainty analysis performed in section 3 carries this entire correction term as an uncertainty.

The LABB is a wedge cavity design, considerably larger, but otherwise similar in its basic design to the OBC, but with selectable temperature between 190K and 360K. During TVAC testing it was located at a distance of 11.5" from the scan mirror. At this position its entrance aperture is large enough to fully contain four consecutive AIRS footprints. The walls of the LABB are coated with Aerogalze Z-302, which has a reflectivity of less than 0.11. For the wedge angle of 27.25 degrees and the AIRS geometry more than 6 specular reflections are required before the beam exits the cavity. The LABB emissivity is theoretically better than $(1-(0.11)^6)$, i.e. better than 0.9999. The LABB output is given directly by the Planck function corresponding to its temperature. The Platinum Resistance Thermometers (PRT) were NIST calibrated. The LABB output is thus NIST traceable through contact thermometry, but not through actual radiance measurements.

A.3.3 Instrument Polarization and Scan Angle Dependence

A.3.3.1 Measured Polarization

Polarization data were obtained during system level testing in Thermal Vacuum of the AIRS instrument polarization. An off-axis section of a paraboloidal mirror is used to project the image of a target aperture onto the field stop of the AIRS instrument. The polarization of the optical beam entering the AIRS entrance pupil has four possible states, selectable by a choice of one of four positions of a filter wheel containing wire grid polarizers in three different orientations, plus one open position. The filter wheel is in close proximity to the target aperture, reducing the clear aperture requirements on the polarizers. The polarizers and the targets are actively cooled with liquid nitrogen to a temperature less than 150 K to reduce the effects of thermal background signal on the polarization measurements..

Figure A3.3 shows the measured polarization obtained during T/V testing (Ref.8). The measured data show very good correlation with a theoretical calculation of the polarization based on first principles. The theoretical polarization is based on component measurements of S and P transmission and reflection made on witness samples during the development phase. Grating polarization was calculated using a numerical electromagnetic model. Mirror data were obtained

from MIT Lincoln Labs (Ref.9). The system polarization model uses these data in a Mueller matrix formalism to arrive an overall determination of the system polarization. We do see some departure in the longer wavelengths from the theory. This deviation is included in the uncertainty modeling.

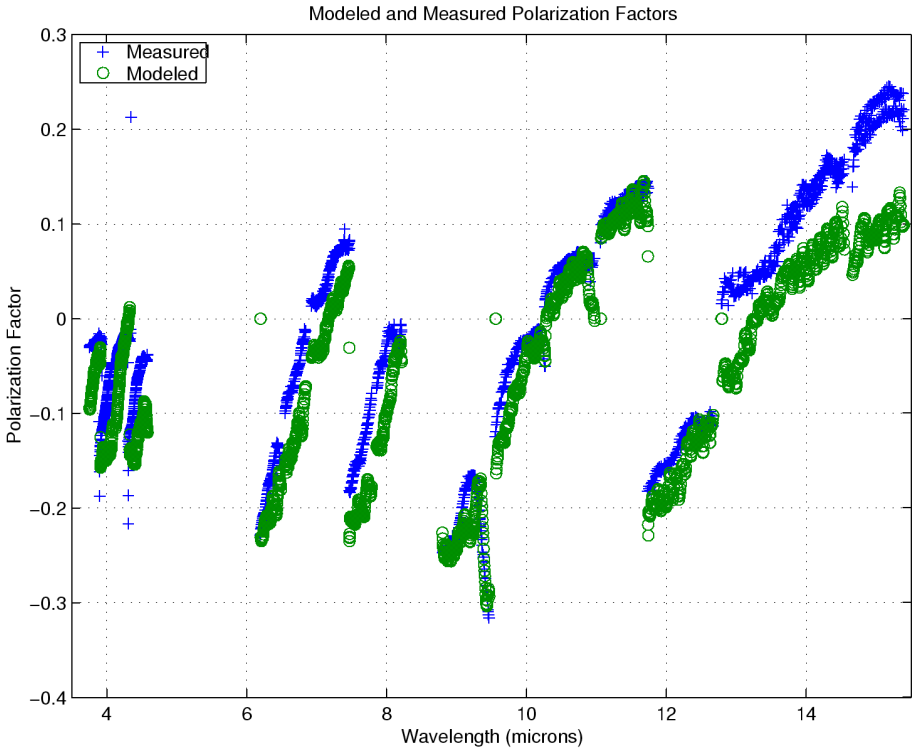

Figure A3.3. Measured (blue cross) and modeled (green open circles) polarization for the AIRS instrument.

Figure A3.4 shows the scan mirror polarization data obtained from MIT Lincoln Labs and the derived spectrometer S and P transmission. The transmission of the spectrometer is based on the first principles model, but corrected for the measured polarization of the system. It is this coupling of the scan mirror and the spectrometer polarization as the orientation of the scan mirror changes that produces the scan angle dependence.

Figure A3.5 shows the results of converting the measured and modeled polarization to $p_r p_t$ product using the MIT mirror data. We overlay with this the $p_r p_t$ as calculated from the radiometric intercept at nadir and 40° scan angles as described in section A3.1, step 1. The radiometric data confirms the polarization data and model an gives us 4 data sets from which to determine the $p_r p_t$ term. We have chosen to use the average of the measured and modeled data sets as our at-launch $p_r p_t$ values. We carry the difference of these two sets as the uncertainty.

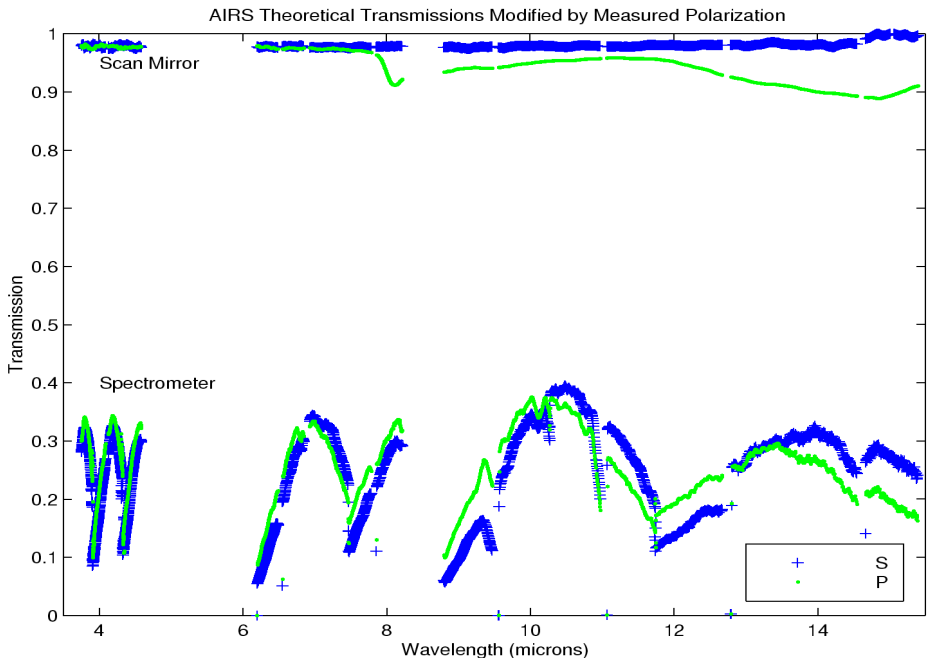

Figure A3.4. Measured scan mirror polarization and modeled transmissions modified by the measured polarization. The green (thin) curve is the P-polarization.

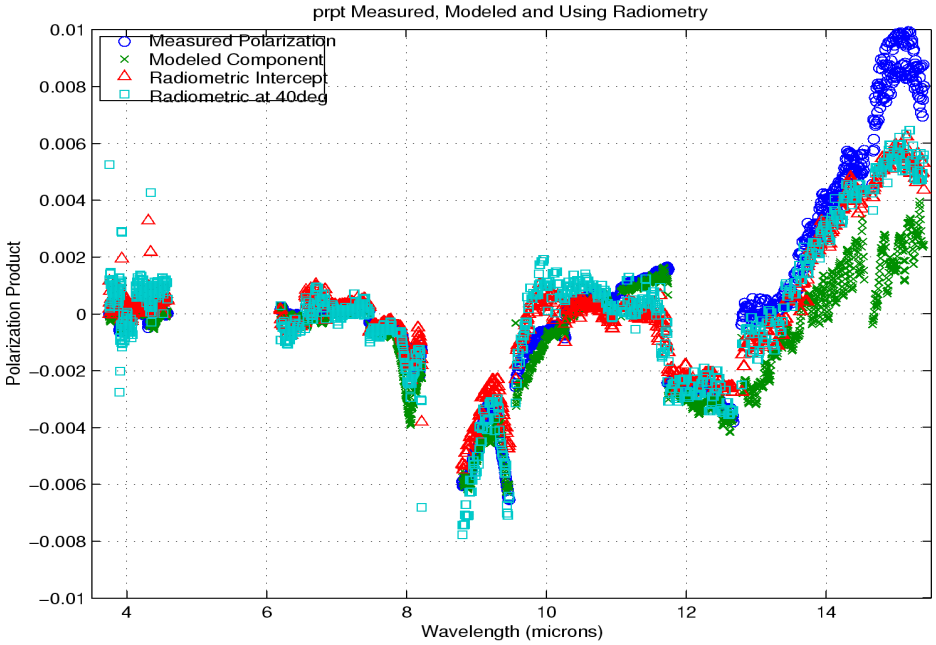

A3.5. Polarization product, $p_t p_t$ obtained 4 different ways. The average of measured and modeled is used in the at-launch L1B for scan angle dependent correction.

A.3.3.2. Measured Scan Angle Dependent Radiometric Correction Term

Measurements were obtained on the AIRS scan angle radiometric response in its final flight configuration. The AIRS instrument was allowed to view the Large Area Blackbody (LABB) at scan angles from about −48° to +36°. The radiometric offset was calculated as the difference between the radiance as derived using the internal On-Board Calibrator Blackbody (OBC), and the known radiance of the LABB.

$$N_{p\_meas} = \quad N_{calc} - N_{calc,nadir}$$

The derived (calculated) radiance for the LABB from the AIRS measured digital number was obtained using the measured dn's and averaging over all scans. The temperature correction was then calculated from the radiometric offset.

$$\Delta T = \frac{N_{p\_meas}}{\P N / \P T}$$

The comparison between the modeled and measured scan angle dependence is shown in Figure A3.6. We see good correlation for most scan angles and channels indicating we have low residual errors.

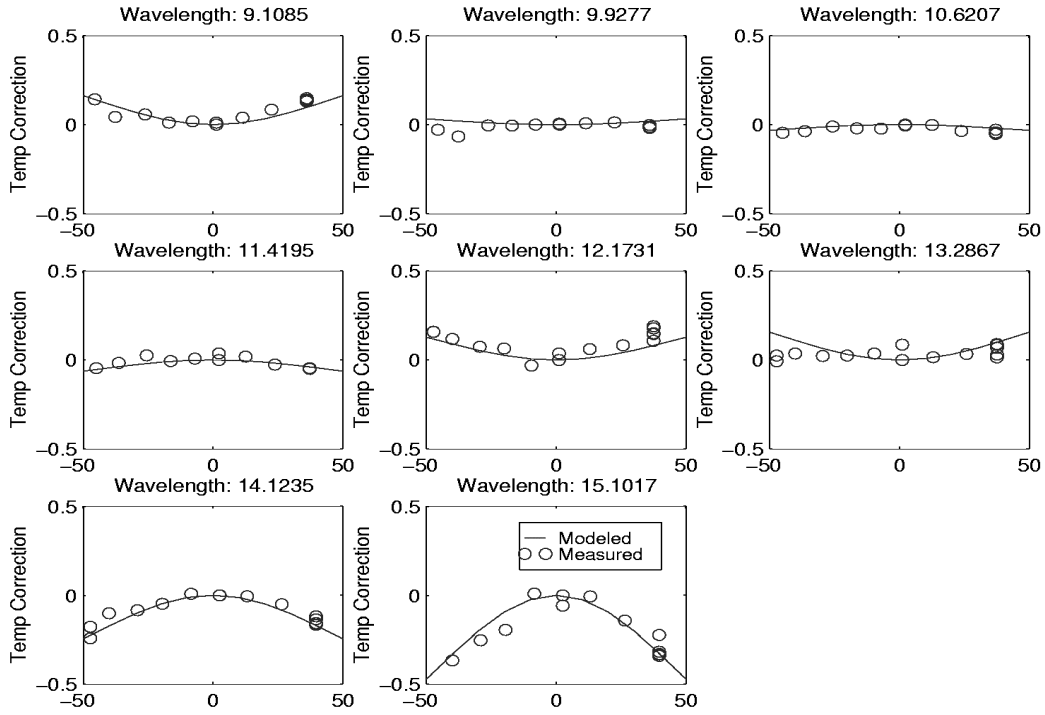

Figure A3.6. Scan angle dependent radiometric offset for the longest wavelength center module reference detectors.

A3.4 Scan Mirror Nonuniformity Uncertainty

The AIRS scan mirror emissivity (averaged over the AIRS spectral coverage) is 0.015, with an estimated rms variation of less than 0.0005. The AIRS radiometric calibration uses different parts of the scan mirror for the scene, the space view and the OBC view.

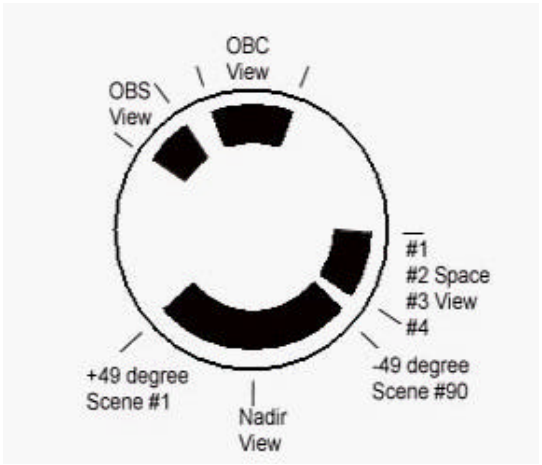

Figure A3.7 The scan mirror rotates through 360 degree every 2.667 seconds, producing one scan line with 90 footprints on the ground and 6 calibration related footprints. Different parts of the scan mirror (highlighted in black for arrays M11 and M12) are used for calibration views and scene views. Arrays M5 through M12 use the outer part of the scan mirror, while arrays M1 through M4 use the center part.

During the pre-launch calibration a scan angle dependent correction term was measured which included polarization and any scan angle dependent emissivity effects. No emissivity effects were detectable, since the observed scan angle dependence agreed typically to within 0.1K with the prediction based on polarization alone.

After some time in orbit the emissivity of the scan mirror may differ from the pre-launch calibration values. Water ice deposits are not an issue, since they do not stick in the vacuum at 250K scan mirror temperature. Molecular contaminants is the most likely cause of emissivity degradation. It is estimated that after five years on orbit (nominally the End of Life, EOL) the layer of molecular contaminants on the scan mirror will be 100A thick, increasing its emissivity by 0.01 to 0.025. Since the mirror is protected inside the rotating barrel baffle, there is no preferred area of exposure to deposits. We therefore expect the 100A thick layer to be very uniform in thickness.

The following section gives the derivation of the correction term and a worst case estimate of the magnitude, assuming a 100A thick layer with a 10% variation in contaminant thickness. This variation in emissivity would cause an rms emissivity variation of 0.001. The analysis shows that the resulting emissivity correction is small.

A3.4.1 Derivation of the correction term.

We express true radiance from the scene, $N(\delta)$, as the sum of the scan angle emissivity independent term , No, a correction term, $\Delta N(\delta)$,

$$N(\delta) = No + DN(\delta)$$

Assume that the scan mirror emissivity seen by a detector at scan angle δ relative to nadir is $e(\delta)$. There are 90 scene views at scan angles $-49 < \delta < +49$ degrees, space view occurs at scan angle δ=s, and the OBC is viewed at scan angle δ=b. The reflectivity of the scan mirror is $r(\delta)=1-e(\delta)$. The signal $N(\delta)$ from the scene then gives the output:

$$V(\delta) * a_1 = N(\delta)*r(\delta) + e(\delta)*N(s) + Xo$$

where a_1 is the gain and we neglecting the small polarization offset and non-linearity terms. The space view signal due to the scan mirror emissivity and other background or electronic offset signals, *Xo*, is

$$V(s) * a_1 = N(s)*e(s) + Xo,$$

The view at the calibration blackbody produces the signal:

$$V(b) * a_1 = N(b)*(1-e(b)) + e(b)*Ns + Xo.$$

Combining the equation

$$(V(\delta)-Vs)/ (Vb-Vs) = (N(\delta)*(1-e(d)) + Ns(e(d)-e(s)))/(Nb*(1-e(b)) + Ns(e(b)-e(s)))$$

and noting that $e(\delta) << 1$ and $Ns * (e(b)-e(s)) / Nb << 1$ with the cold scan mirror we find

$$DN(\delta) = Ns * (e(s)-e(\delta)) - No * (e(b)-e(\delta)).$$

As a check of the equations, note that if the scan mirror emissivity is uniform, i.e. $e(\delta)=e(s)=e(b)$, then $DN(\delta)=0$, i.e. the correction term vanishes for all δ.

A3.4.2 Estimate of the magnitude of the correction term DN.

The panel in Figure A3.8. shows the assumed conditions for the change between the pre-launch/begin of life and end of life conditions with respect to scan mirror temperature, average emissivity of the scan mirror for scene view, OBC view and space view, respectively, based on the assumed worst case 0.001 variation of the scan mirror emissivity.

Since retrievals are carried out in terms of brightness temperatures, we express the scan mirror emissivity variation dependent correction term *DN* as a temperature correction *DT*. This is shown in Figure A3.3. as function wavelength and scene temperature . At brightness temperatures of 235 K and warmer the magnitude of the correction term is less than 0.15K. At lower temperatures the correction is somewhat larger. The AIRS level 1b processing neglects this term. The term is therefore included it in the overall radiometric uncertainty estimate.

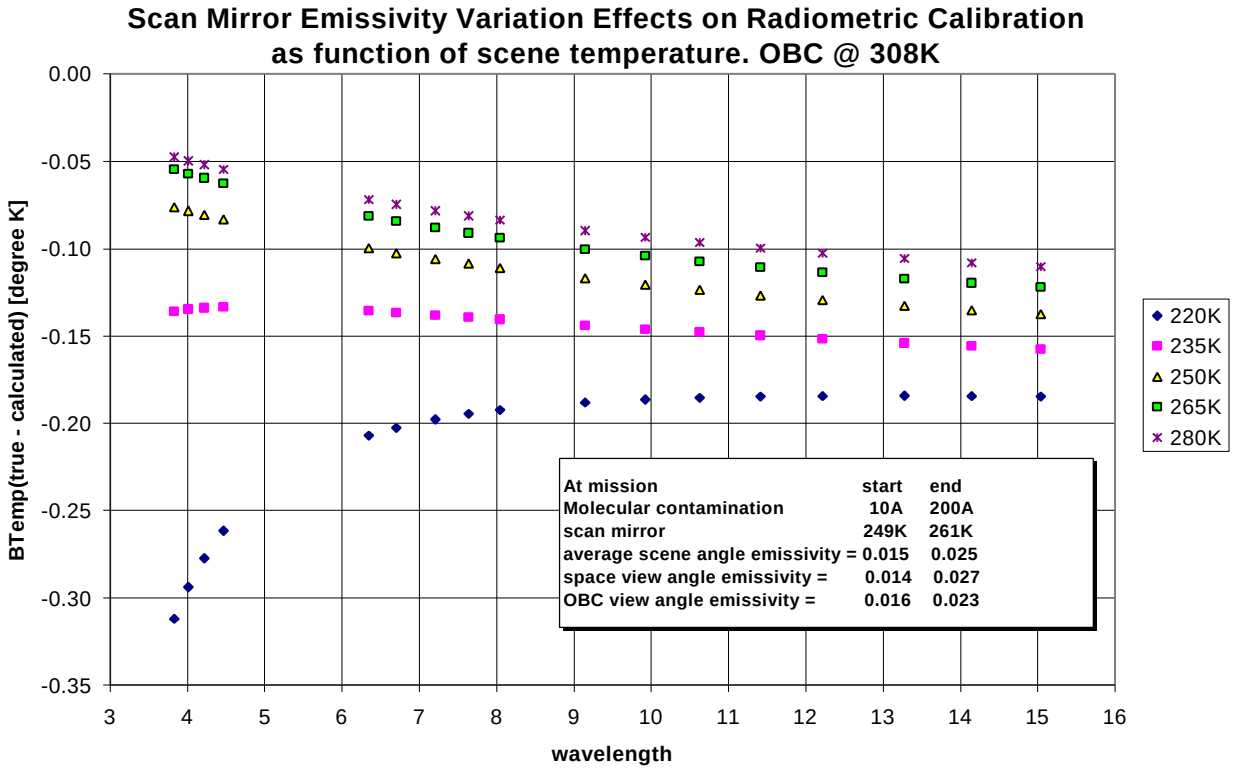

Figure A3.8. Effect of scan mirror emissivity variation on calibration between characterization pre-launch and end-of-life (which is degraded by contamination) for a worst case emissivity variation of 0.001. The differences at temperatures above 235K in the 0.05 to 0.1K class.

Appendix 4. Determination of the SRF centroid model parameters

The determination of the SRF centroid model parameters was a pre-paunch TVAC calibration activity. The AIRS pre-launch spectral calibration utilized a novel approach: The output of a high spectral resolution laboratory grade Michelson interferometer (Ref.10) was directed into the AIRS entrance pupil. Optical path difference in the Michelson interferometer was stepped from +2.88 cm to -2.88 cm synchronously with AIRS data collection. Each AIRS detector thus produced an interferogram, the Fourier transform of which is the spectral response function (SRF) for that detector. Absolute wavenumber calibration was achieved by placing a gas cell containing low-pressure carbon monoxide between the interferometer and AIRS, which superimposed several carbon-monoxide absorption lines onto several SRF's in the 2100 cm-1 spectral region. This technique produces a calculated SRF centroid for each detector, for each run of the stepping interferometer.

The data fitting process was carried out in two steps. First for each detector array, the two unknown quantities y^k_o and F_k were chosen to minimize the difference between the model centroids (Eq. 4.4) and the measured centroids, in a least-squares sense. The residuals between measured and modeled channel centroids were observed to exhibit some small systematic errors for some arrays, with a maximum error corresponding to 1-2% of the FWHM. A quadratic correction using a_k removed this small systematic error on an array-by-array basis. The very small a_k correction term ranges from $-1.2*10^{-05}$ to $+1.4*10^{-05}$.

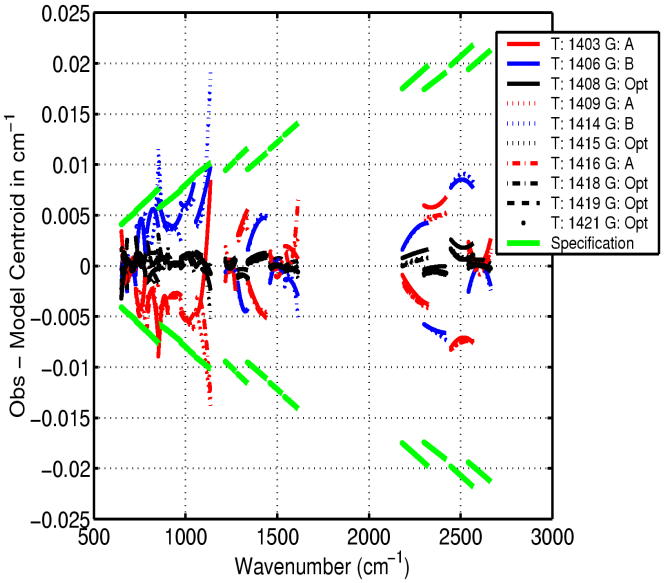

Figure A.4.1 SRF centroid residuals in wavenumber units relative to the mean of all tests at T = 161 K. The green lines bound the permissible 1% of SRF width maximum permissible deviation.

Figure A.4.1 highlights the sensitivity of the spectral calibration test setup and the high signal-to-noise of these measurements. The array position were found to vary slightly with temperature by an amount equivalent to a centroid shift of 2.2% of a width per K. No change was detected in the effective focal lengths, F_k as function of temperature between 149K and 161K. Because the spectrometer temperature is actively maintained to within 30mK, the effect in orbit of temperature variations on the SRF centroid will be negligible.

The SRF width and shape for a grating spectrometer are frozen into the design by the grating, the grating illumination defined by geometrical and diffraction effects, the detailed properties of the order isolation filters and by the effective focal length F_k of the Schmidt mirror. The low-level, far-out-of-band response of the SRF, critical for separating the radiative contribution of the surface from that of the lower atmosphere, is determined entirely by the details of the grating and the focal plane, independent of system linearity or scene illumination. The measurement of the SRF shape turned out to be the most challenging part of the AIRS pre-launch calibration effort. The SRF width measurements showed no variation with temperature, and were determined to the required specs (1-3%) or better.

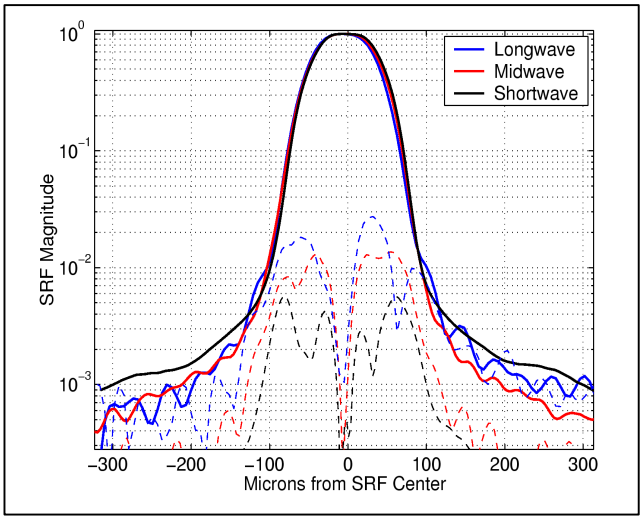

Figure A.4.2 shows measured SRFs averaged over three broad wavenumber ranges. These are averages of channels over five arrays on average, shortwave, midwave and longwave. The SRFs are nominally 100 microns wide, so this figure shows that the SRF magnitude at 3 full SRF widths from the channel center is below 0.1% of its peak value.

The observed SRFs were fit to a simple analytic function (roughly the sum of a Lorentz plus a Gaussian shape) with good results. Our main goal for these fits was to smooth noise in the SRF wing. These fits included the effects of the interferometer, which introduces very noticeable sinc-function ringing in the longest wave arrays. Variations of the SRFs within a single array were undetectable and below our specifications, allowing us to use a single shape (but not width) for each channel in each array. Variations in the SRF shape among arrays were also quite small, but big enough to be explicitly included in the calibration.

Appendix 5. Temperature change which corresponds to a 1% change in radiance

Table A.5.1. Temperature change which corresponds to a 1% change in radiance.

Temperature change equivalent for a flux increase of							1	%		
	mean			Scene Temperature [degree K]						
array	array	205	220	235	250	265	280	295	310	325
name	microns									
M1a	3.8267	0.11	0.13	0.15	0.17	0.19	0.21	0.23	0.25	0.28
M2a	4.2196	0.12	0.14	0.16	0.18	0.21	0.23	0.25	0.28	0.31
M1b	4.0125	0.12	0.13	0.15	0.17	0.20	0.22	0.24	0.27	0.29
M2b	4.4678	0.13	0.15	0.17	0.19	0.22	0.24	0.27	0.30	0.33
M4a	7.2063	0.21	0.24	0.28	0.31	0.35	0.39	0.43	0.48	0.53
M4b	6.3469	0.18	0.21	0.24	0.27	0.31	0.34	0.38	0.42	0.46
M3	6.7002	0.19	0.22	0.26	0.29	0.33	0.36	0.40	0.45	0.49
M4c	7.6333	0.22	0.26	0.29	0.33	0.37	0.41	0.46	0.51	0.56
M4d	8.0403	0.23	0.27	0.31	0.35	0.39	0.44	0.48	0.53	0.59
M5	9.1435	0.27	0.31	0.35	0.40	0.44	0.49	0.55	0.61	0.66
M6	9.9200	0.29	0.33	0.38	0.43	0.48	0.54	0.59	0.65	0.72
M7	10.6300	0.31	0.36	0.41	0.46	0.51	0.57	0.63	0.70	0.77
M8	11.4108	0.33	0.38	0.43	0.49	0.55	0.61	0.68	0.75	0.82
M9	12.2141	0.35	0.41	0.46	0.52	0.59	0.65	0.72	0.80	0.87
M10	13.2723	0.38	0.44	0.50	0.57	0.64	0.71	0.78	0.86	0.94
M11	14.1455	0.41	0.47	0.53	0.60	0.67	0.75	0.83	0.91	0.99
M12	15.0336	0.43	0.50	0.57	0.64	0.71	0.79	0.87	0.96	1.04

Appendix 6. Level 1b Validation: Routine Radiometric Bias Estimation.

This section addresses the validation of the AIRS Level 1B calibrated radiances, with an emphasis on radiometry. The radiometric and spectral calibration of AIRS is discussed in some detail in the AIRS Instrument Calibration Plan and in the main body of the AIRS Level 1b ATBD. In this appendix we show how calibration will be validated and monitored by globally evaluating AIRS radiometric biases. The concept is illustrated with an example from HIRS/2 radiometric bias monitoring, where as little as 0.1K bias is detectable.

For AIRS field-of-view which are free of clouds, the AIRS Radiative Transfer Algorithm (RTA) can be used to calculate I_{calc}, the "upwelling radiance" or "clear column radiance" in each of the 2378 AIRS spectral channels. The four main components of the upwelling radiance are surface emission, atmospheric emission, reflected thermal downward-flux and reflected solar flux. If we assume that the state of the atmosphere, described by the temperature profile, T(p), the moisture profile q(p), and the surface temperature and emissivity, T_s and ε_s, is defined by the forecast model in a global GCM, then the statistical analysis of the difference between the calculated radiances, I_{calc}, and the observed radiances, I_{obs}, provide a measurement of the bias.

The bias may be due to one or more of the following:

1. the inability to accurately calculate I_{calc}, due to uncertainties in the radiative transfer physics, i.e. line strengths, line shapes, the effect of foreign broadening on line width, etc. or
2. a bias was introduced in I_{obs} in the process of cloud-clearing or due to cloud contamination in the case of hole-hunting, or
3. instrumental artifact, such as inadequately known spectral response or radiometric calibration function, possibly due to long-term changes in instrument characteristics.

Accurate estimation and elimination of the bias is critical to the success of the retrieval process and direct assimilation. Define a channel dependent bias correction function

$$B = I_{obs} - I_{calc}$$

which is evaluated using a large number "truth data", i.e. "cloud-free" footprints where the state of the atmosphere is "assumed" to be known. The observed bias for each truth point is expressed as a channel dependent bias equation

$$B = a + b*I_{obs} + c*\cos^{-1}(\theta) + d*T_s + e*Q + \ldots,$$

where θ is the slant path angle. T_s is the surface temperature and Q is the water vapor column, obtained from a short term forecast or approximated using other channels from the same

footprint. The retrieval and/or direct assimilation of the data then use the bias corrected "tuned" radiance

$$I_{tuned} = I_{obs} + B.$$

While the quantities *a, b* and *c* in the bias equation have the appearance of instrumental offset and gain errors, they and the other terms may in fact be due to the combination of residual instrumental effects and approximations in the radiative transfer algorithm. Lapse rate, sun angle, latitude and land/ocean dependencies are additional terms frequently included in the bias equation. The bias equation coefficients are determined from the truth data set in a least squares sense. For AIRS there may be enough redundancy in the 2378 spectral channels to separate instrumental and spectroscopic effects.

The are two approaches to collecting the truth data sets to monitor the bias on an operational basis:

a) The approach developed during the last two decades for the TOVS uses the operational radio sondes launched by the various national meteorological services. Since only about 30 of the 5000 routine radio sonde launches per day are coincident within a 2 hours time and 100 km position window with the satellite overpasses and are cloud-free, it requires several months of data to reliably evaluate the global bias. The accuracy of the bias determination is limited by the accuracy of the radiosondes, assuming that the spatial and time mismatch between the satellite overpass and the radio sonde launches averages out. This approach will be used by the NOAA/NESDIS affiliated AIRS team members for operational bias monitoring.
b) The second approach to evaluate the bias is to "tune using the forecast". If one assumes that the analysis GCM model (or three hour forecast), which is based on ingesting all radiosonde and satellite data, is globally unbiased and accurate, then the statistical evaluation of ($I_{obs} - I_{calc}$) for all footprints which are cloud-free yields the desired bias values. This allows the estimation of the bias using as little as one day's worth of data. This approach works for bias evaluation only if the data being evaluated are not used to a significant extent in the definition of the forecast. Otherwise the tuning process may lead to unexpected instabilities.

Figure A.6.1. shows a typical example of bias monitoring relative to the forecast using the NOAA 14 HIRS channel #6 at 13.64 microns by ECMWF for clear, ice-free ocean for the 30 days from September 19 through October 19, 2000 (Tony Hollingsworth, ECMWF, private communication). This HIRS channel, which is sensitive to mid-tropospheric temperature, is not used in the ECMWF assimilation. The vertical scale is the brightness temperature bias in degree K. The 2rd curve from the top (solid blue) is the mean value of ($I_{obs} - I_{calc}$), which fluctuates within 0.1K around +0.2K. The 3nd curve from the top (solid red) is the mean residual bias, after bias correction using a bias equation. It residual fluctuates within 0.1K around +0.1K.

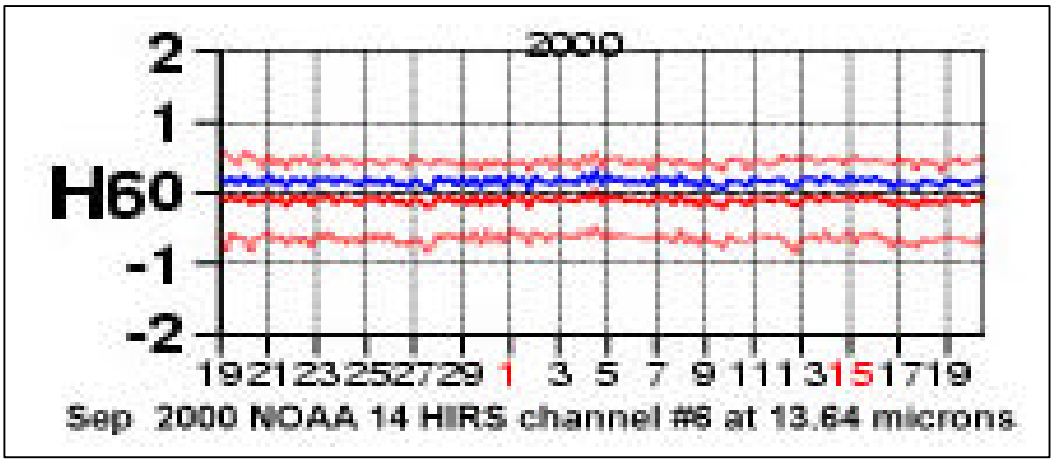

Figure A.6.1. shows a typical example of bias monitoring relative to the forecast using the NOAA 14 HIRS channel #6. Note that bias as little as 0.1K can be tracked.

This example shows that

a) the HIRS#6 calibration bias of 0.2K in the 240K to 260K range is excellent, corresponding to only 0.3% of the signal amplitude.
b) the ECMWF bias estimation methodology is capable of estimating a radiometric bias as low as 0.1K. This is an important diagnostic capability, given that the AIRS radiometric calibration residual error are typically 0.1K or less.

Monitoring AIRS radiometric bias using the forecast is an activity of NOAA/NCEP associated AIRS science team members. Bias estimation and elimination demands instrument stability on a months timescale, assured by the a-thermal design of AIRS and the absence of critical parts moving with interferometric precision. The standard deviation of (observed-bias_adjusted_calculated), shown in the 1st and 4th curves (dotted red lines) in Figure A.6.1. is 0.6K. This is much larger than the 0.2K noise for each HIRS#6 footprint. The most likely cause for this is a combination of cloud contamination of assumed cloud-free footprints, possible uncertainties in the HIRS SRF used for the radiometric transfer calculations, and/or disagreements between the upper tropospheric temperature measured by HIRS#6 and found in the short-term forecast. Analysis of the bias and standard deviation as function of SRF centroid position and correlation to the spectral contrast in the upwelling radiance will be diagnostic of the origin of the bias.

Appendix 7. Validation of Level 1B Spectral Radiances

A.7.1 Background

This section addresses the validation of the AIRS Level 1B calibrated radiances, with an emphasis on their spectral nature. The radiometric and spectral calibration of AIRS is discussed in some detail in the AIRS Instrument Calibration Plan and in the main body of the AIRS Level 1b ATBD. The term spectral calibration refers to our knowledge of the AIRS spectral response functions (SRFs), which includes their shape, spectral location (centroids), and how these quantities change with temperature and AIRS focus.

Validation of the AIRS Level 1B radiances involves not only validation of the radiometric accuracy of these radiances, but also validation of the SRFs that gives AIRS its high spectral resolution. AIRS Level 2 retrievals use a fast radiative transfer model (AIRS-RTA) to minimize the differences between the observed and computed radiances. Since the forward model is very sensitive to the exact form of the AIRS SRFs, we consider the validation of the SRFs part of Level 1B validation. Although extensive ground calibration of AIRS has given us much information on the form of the SRFs, they cannot be known exactly until AIRS is in orbit for reasons described later. (See the AIRS Level 1 ATBD for details on in-orbit spectral calibration).

The validation of the AIRS spectral calibration will rely on comparisons between observed and computed radiances, so it will also involve simultaneous validation of the forward model spectroscopy and the fast radiative transfer parameterization. Separately validating the various aspects of the Level 1B radiances (*i.e.*, radiometric calibration, SRF knowledge, spectroscopy, fast model parameterization) will require a wide range of inter-comparisons under many atmospheric conditions. Although it may appear difficult to separate out these various effects, the copious redundancy (in terms of weighting functions) in the AIRS spectral channels, coupled with good models for instrument errors and spectroscopic errors, should allow us to de-couple these effects and separately validate them in large part.

Validation of the AIRS radiometric calibration is partially addressed here, but is also covered in the validation of sea-surface temperature products. AIRS sea-surface radiances provide the best opportunity for validation of the components of the AIRS absolute radiometric calibration that are common to all detectors, such as the temperature/emissivity of the on-board blackbody calibrator (OBC) and scan mirror angle effects. The spectral validation activities discussed in this section will depend in-part on validation of the absolute radiance calibration (at least for high radiance scenes) via observations of well characterized surface sites such as the sea-surface.

Conceptually, AIRS convolves the Earth's up-welling monochromatic radiances with the AIRS SRFs. The earth view detector counts are converted into radiances in the standard way using detector space view counts and on-board blackbody calibrator (OBC) view counts recorded in-

between each scan line. These measurements, combined with the OBC temperature, provide the basic radiometric calibration of AIRS. Early ground calibration results generally suggest that the OBC illumination of the detector focal plane is quite uniform, that the detector responses are very nearly linear, and that scan angle effects are relatively small. Consequently, we hope that absolute radiometric calibration and validation will primarily be involved with characterizing the OBC temperature and stability, which are essentially independent of spectral channel.

The overall goal is to validate and possibly improve our *models* of the AIRS instrument behavior, the AIRS-RTA, and the spectroscopy in the AIRS-RTA and in doing so validate the AIRS Level 1B radiances. Since these models are largely independent of scan angle and cloud amount, this process will concentrate on nadir views of fields deemed very clear. Figure 1 illustrates the basic flow of information in the Level 1B validation, highlighting the comparison of computed and observed radiances in the ``Radiance Residual Analysis'' box.

Figure 1: Top level diagram of the AIRS Level 1B validation process.

A.7.2 AIRS Instrument Spectral Model

AIRS has 2378 spectral channels that reside on 17 different linear detector arrays. Each detector serves as an exit slit for the AIRS grating spectrometer. AIRS uses 11 entrance slit apertures, which means that some arrays use the same entrance slit. The 2104 channels above 729 cm^{-1}, which are photo-voltaic (PV) detectors, consist of redundant pairs, giving a total of ~ 4500 channels. The detectors below 729 $cm^{-1}$are photo-conductive detectors with no redundancy.

The AIRS instrument spectral model has three basic components, the grating model, the SRF shape, and the entrance filter fringe positions, which combined together are used to simulate AIRS radiances and to build the fast model (AIRS-RTA).

Grating Model: As discussed in the AIRS level 1b ATBD, a relatively simple model based on the standard grating equation is able to model the AIRS wavenumber scale, at least on a per array basis. This model gives us the ability to predict the SRF centroids for each detector within an array given knowledge of the centroid of at least one detector on that array. The dependence of the grating model on both the instrument temperature, and focus, will be determined from ground calibration data. Once in orbit, up-welling radiances will be used to determine the absolute wavenumber positions of a sub-set of detectors. This information, combined with the grating model, will then allow us to determine the centers of every AIRS detector. Several arrays do not sense sharp, profile independent, features in the up-welling radiances, so we will have to use the grating model to transfer absolute calibration from one array to another. Since the focal plane is a rigid entity, this transfer should be highly accurate.

SRF Shape: The shape of the AIRS SRF is determined by a combination of the grating resolution, dispersion, size of the entrance slit apertures and the detector widths, and instrument scattering (important for the low-level SRF response). Extensive ground calibration tests enabled reasonably accurate measurements of the shape of all ~ 4500 channels, with some signal-to-noise limitations for the long-wave arrays. A simple analytic model has been developed that appears to have sufficient accuracy to model all the grating spectrometer SRFs with just a few parameters per array. In addition, the change in the SRF width with de-focus has been measured during ground calibration. In the improbable case that AIRS suffers any significant de-focus during launch, the SRF widths can be estimated from the absolute wavenumber calibration via the grating model we have developed. It will be very difficult to calibrate the grating spectrometer SRF shape (SRF width, wings) in orbit. We can only determine if the AIRS radiances are consistent with our estimate of their in-orbit shape.

Fringes: The detailed shape of the AIRS SRF is defined by the product of the smooth SRF's generated by the grating spectrometer times a channel spectrum function. The channel spectrum

is due to channel spectra (fringes) in the entrance slit aperture filters, $F_k(\nu,T)$. $F_k(\nu,T)$ is a analytic function describing the channel spectrum for the k'th array at frequency ν and temperature T. Most of these 11 filters have some spectral regions containing interference fringes. These fringes have a nominal spacing (free spectral range) of 1.2 cm^{-1}, and a contrast of up to ±5% max. The fringe spacing is small enough to potentially impact all of the AIRS SRFs. Define $SRF\_smooth_k(\nu, \nu_o)$ as the ``pure" grating spectrometer function of a detector on array k, with centroid at frequency ν_o. Then the SRF used in the forward algorithm is given by

$$SRF(\nu, \nu_o) = F_k(\nu,T) * SRF\_smooth_k(\nu, \nu_o).$$

As part of the spectral calibration the function $SRF(\nu, \nu_o)$ has been measured at 149K, 155K and 161K. The positions of the peaks of the entrance aperture fringes are sensitive to temperature via the index of refraction of the filter's germanium substrate. The fringe peaks shift the equivalent of -9.96 microns/degK, while the SRF centroids shift –2.7 microns/degK. The temperature of the entrance filters is measured with 0.01K resolution with a thermistor.

Since the width of the SRF is 100 microns (in focal plane coordinates), a change of 0.1degK in spectrometer temperature corresponds to a shift of the fringe peaks of 1% of the SRF. Consequently, the fringes will effectively be frozen relative to the SRFs once the AIRS has temperature stabilized in orbit to within 0.1K of the setpoint of the spectrometer thermostat.

The temperature dependence of $F_k(\nu,T)$ was verified and the shape of $F_k(\nu,T)$ was determined. Given the shift in the "phase" of the channels spectra by -9.96 microns/degK, the function $F_k(\nu,T)$ can be calculated at any temperature in the 149K to 161K range.

The fringe shift of -9.96 microns/degK allows the positions of the fringes relative to the SRF centroids to be validated in orbit, by measuring the ratio of the detector gain at two temperatures. Initial tests to verify this were carried out during TVAC. The 2.8 watt choke heater in the spectrometer will be used to increase the spectrometer by 5K. A test to verify this is planned during the on-orbit checkout phase, where the choke heater will be used to shift the spectrometer by +/- 2.5K around its nominal value. The pre-launch verification of this test will be carried out during system integration TVAC at TRW.

A.7.3 Spectroscopy, kCARTA, AIRS-RTA

Comparisons of observed and computed AIRS Level 1B radiances depends on the accuracy of the AIRS spectral calibration and on the accuracy of the spectroscopy used in the computation of the simulated radiances. The accuracy requirements for the AIRS radiative transfer model are demanding, and will require the best available spectroscopy and line-by-line codes. In addition, the

speed requirements for the Level 2 retrievals requires the use of a fast radiative transfer model (which we call the AIRS-RTA) that is based on parameterizations of atmospheric transmittances suitably convolved with the AIRS SRFs. This parameterization is discussed in some detail in the Level 2 AIRS ATBD.

The spectroscopy used in the AIRS-RTA is derived from kCARTA (kCompressed Atmospheric Radiative Transfer Algorithm), which is a monochromatic radiative transfer code based on compressed look-up tables of atmospheric transmittances. These look-up tables are created using a very accurate, but slow, line-by-line code developed at the University of Maryland Baltimore County, called UMBC-LBL. UMBC-LBL is a state-of-the-art line-by-line algorithm that includes features not found in other line-by-line codes such as P/R branch line-mixing in CO_2.

kCARTA will be used as the AIRS reference radiative transfer algorithm. kCARTA's primary purpose is for the generation and validation of the AIRS-RTA. However, it will also be useful for (1) early validation of the AIRS Level 1B radiances before the AIRS channel center frequencies have stabilized, (2) testing effects of new spectroscopy on AIRS simulated radiances for possible inclusion in the AIRS-RTA, and (3) providing AIRS radiances convolved with trial SRF models that are needed for Level 1B validation.

We independently validate the line-by-line algorithms by comparisons with new, better laboratory data when available. kCARTA is validated by comparisons to other line-by-line codes (GENLN2, LBLRTM) and by using it to compute validated radiances measured by the HIS/NAST-I instruments that fly on NASA's ER-2.

The AIRS-RTA is validated before launch by comparing radiances it produces to those computed with kCARTA, using an independent set of profiles (profiles other than those used to perform the regressions for the fast model parameters). The AIRS-RTA is dependent on a proper statistical selection of profiles used in the transmittance regressions (see the AIRS Level 2 ATBD for details). If comparisons of radiances computed with the AIRS-RTA disagree with kCARTA computed radiances when using profiles from actual AIRS retrievals, then our regression profile set must be re-examined. Because both the atmospheric spectroscopy and the AIRS instrument model (SRFs) are fixed in the AIRS-RTA, it cannot be used for some validation activities.

A.7.4 Validation Approach

The basic approach to Level 1B validation is to use independent estimates of the atmospheric state to compute simulated AIRS observed radiances, and compare these with the observed radiances. Our overall goal is to improve the instrument, radiative transfer, and spectroscopic *models* in reasonable, understandable ways in order to reduce the radiance residuals. Since these

models are largely independent of scan angle and cloud amount, this process will concentrate on nadir views of fields deemed very clear.

There is a high level of redundancy in the AIRS channels in the sense that many channels have very similar forward model weighting functions. The retrieval algorithms only use several hundred AIRS spectral channels, generally those with narrow weighting functions in regions where a single gas dominates the radiance. This leaves many channels with somewhat wider weighting functions that probe the same part of the atmosphere as a combination of channels used in the retrieval.

parameterization, (4) behavior of the instrument model if inadequately characterized, and (5) uncertainties (and global variations) of atmospheric gases, such as CO_2, CH_4, and N_2O.

This process will start very early in the deployment of AIRS by comparing observed radiances with radiances computed using climatology. This type of validation will only detect rather severe instrument errors and glaring software bugs. As time progresses we will use ever better independent estimates of the atmospheric state as input to our computed radiances for comparison with the AIRS observed radiances. This includes profiles from (1) the NCEP or ECMWF analysis, (2) AMSU retrievals once they are available, (3) operational radiosondes, (3) special radiosondes launched during the time of AIRS overpasses, (4) ARM site data, and finally (5) intensive in-situ campaign data. As the quality and amount of in-situ profile data improves, our validation analysis will also become more statistical in nature. For example, validation of radiances sensitive to lower tropospheric water vapor are problematic on a case by case basis due to the spatial/temporal variability of water and mismatches between radiosonde locations and the AIRS field of view. However in a large statistical sample of these comparisons the random errors can be greatly reduced.

It may also be possible to validate the instrument model, and some relative aspects of the spectroscopy, by examining the radiance residuals between radiances computed using the Level 2 retrieved profile and observed radiances. The wavenumber dependence of the residuals may highlight slowly varying spectroscopy errors. Instrument model errors (such as incorrect placement of the entrance slit aperture filter fringes) may also be inferred as follows. Perform a series of Level 2 retrievals, each using forward models with different placements of the entrance filter fringe peaks. Then examine the radiances residuals (computed for all channels) as a function of the fringe placement in the forward model and look for patterns that follow the known wavenumber dependence of the fringes. This process would be quite slow since it would most likely require use of kCARTA as the forward model. However, this may be the only way to validate the calibration of the fringe positions.

The AIRS channel center frequencies and the position of the entrance slit aperture filter fringes will not be determined until AIRS is in-orbit. Consequently the AIRS-RTA will not be using the proper instrument model at launch and must be re-computed post-launch once these quantities are determined. This process must be completed as quickly as possible to provide the Level 2 retrieval algorithms with an accurate forward model for the operational products. We will attempt to do as much Level 1B radiance validation as possible during this time frame (using kCARTA) so that the quick production of the new AIRS-RTA will also include any improvements to the spectroscopy and fast model parameterization.

Figure 2 is a more detailed diagram of Level 1B radiance validation. It pictorially shows how the instrument model, spectroscopy, and atmospheric profile information flow into the main validation activity, the analysis of radiance residuals. Note that validation of the AIRS-RTA is done with

kCARTA radiances convolved with the instrument SRF model, and does not require observed AIRS radiances. This step does need to use actual observed (retrieved) AIRS profiles to ensure that a proper statistical set of profiles was used in the development of the AIRS-RTA. The arrows leading to the instrument model from the Level 1A/1B data are calibration activities, and are included here to emphasize that the instrument model will not be complete until AIRS is in orbit.

A.7.4.1 Validation of Radiances Sensitive to Upper Tropospheric Water Vapor

Although Level 1B validation may be successful for many AIRS channels, we expect it will be quite difficult to validate channels sensitive to upper tropospheric humidity, which is very difficult to measure accurately with radiosondes. This will affect a large number of water channels on the M3, M4a and M4b arrays because even if their weighting functions peak at lower altitudes, they have tails at higher altitudes where the radiosonde measurements are extremely inaccurate. Upper tropospheric water radiances are (1) quite low (220 -250K), and (2) offset significantly from the AIRS OBC temperature of 308K and thus are more subject to detector non-linearity errors than other channels. The combination of these problems will make validation of upper tropospheric water vapor radiances difficult. However, the importance of these channels for global climate change and outgoing longwave radiation (OLR), and the fact that AIRS will provide measurements of this key quantity that are far better than existing techniques, should provide impetus for a significant validation effort.

There are two possible approaches to overcome the limitations of the radiosonde network for validation of upper tropospheric water radiances. First, an intensive field campaign is needed that stresses clear sky conditions and has the capability to make in-situ high-altitude water vapor measurements. Since it is difficult for the ER-2 to fly over a range of altitudes needed for in-situ water vapor measurements, our goals would be better served with NASA's WB57 equipped with several in-situ water sensors. Secondly, deployment of a water vapor lidar at a high altitude site, coupled with a microwave radiometer for measurement of the total water burden, could provide validation of upper tropospheric water vapor. A possible candidate site for this lidar would be NOAA's Mauna Lao observatory in Hawaii. Although there are existing lidars at some ARM sites, they have difficulty measuring high altitude water vapor due to the large signal reduction by the intervening lower atmosphere.